MULTIVARIATE PRODUCTION SYSTEMS OPTIMIZATION

A REPORT

SUBMITTED TO THE DEPARTMENT OF PETROLEUM ENGINEERING

AND THE COMMITTEE ON GRADUATE STUDIES

OF STANFORD UNIVERSITY

IN PARTIAL FULFILLMENT OF THE REQUIREMENTS

FOR THE DEGREE OF

MASTER OF SCIENCE

By

James Aubrey Carroll, III

December, 1990

Take heed you do not find what you do not seek.

[English Proverb]

Approved for the Department:

Roland N. Horne

Abstract

The objective of this research has been to investigate the effectiveness of nonlinear optimization techniques to optimize the performance of hydrocarbon producing wells.

The performance of a production well is a function of several variables. Examples of these variables are tubing size, choke size, and perforation density. Changing any of the variables will alter the performance of the well. There are several ways to optimize the function of well performance. An insensible way to optimize the function of well performance is by exhaustive iteration: optimizing a single variable by trial and error while holding all other variables constant, and repeating the procedure for different variables. This procedure is computationally expensive and slow to converge--especially if the variables are interrelated.

A prudent manner to optimize the function of well performance is by numerical optimization, particularly nonlinear optimization. Nonlinear optimization finds the combination of these variables that results in optimum well performance by approximating the function with a quadratic surface. The advantages of nonlinear optimization are many. Using nonlinear optimization techniques, there is no limit to the number of decision variables that can be optimized simultaneously. Moreover, the objective function may be defined in a wide variety of ways. Nonlinear optimization achieves quadratic convergence in determining the optimum well performance and avoids a trial and error solution. Several different optimization methods are investigated in this study: Newton's Method, modified Newton's Method with Cholesky factorization, and the polytope heuristic.

Significant findings of this study are: the performance of Newton's Method can be greatly improved by including a line search procedure and a modification to ensure a direction of descent; For nonsmooth functions, the polytope heuristic provides an effective alternative to a derivative-based method; For nonsmooth functions, the finite difference approximations are greatly affected by the size of the finite difference interval. This study found a finite difference interval of one-tenth of the size of the variable to be advisable.

Acknowledgements

I would like to thank Dr. Roland Horne for providing me with thoughtful guidance, sage advice, and understanding patience. I also extend thanks to Dr. Khalid Aziz for providing sound and judicious counsel and to Dr. Hank Ramey for his generous contributions.

I would like to thank Rafael Guzman for the time he invested proofreading several drafts of this manuscript. I would also like to thank Cesar Palagi, Evandro Nacul, Adalberto Rosa, Michael Riley, and Mariyamni Awang for providing a constant source of quality advice. I would like to thank Russell Johns for providing experience in the drafting of this manuscript. I would like to thank Suhail Qadeer and Daulat Mamora for helping me with the computer hardware and David Brock and Chick Wattenbarger for being of assistance with the computer graphics.

I would also like to express thanks to Dr. Walter Murray and Sam Eldersveld of the Stanford Optimization Laboratory for their accessibility and helpfulness. I would like to thank Dr. Jawahar Barua for writing a superb thesis that was instrumental in my fully appreciating nonlinear concepts. I would like to thank Gunnar Borthne of the Norwegian Institute of Technology and Godofredo Perez of the University of Tulsa for providing me with computer programs that facilitated my work. I would also like to thank Joseph Gump of Chevron, U.S.A., Gene Kouba of Chevron Exploration and Production Services, and Dr. Rajesh Sachdeva of Simulation Sciences for providing me with a great deal of time and help pertaining to system theory. I would like to thank Dr. Parvis Moin of NASA Ames Research Center for inspiring my work by showing me the beauty and simplicity of numerical methods.

I would like to express my sincere gratitude to Dr. Elias Schultzman and the National Science Foundation for providing me with the financial capacity to pursue this research. I would also like to thank the Stanford University Petroleum Research Institute for providing resources and support.

Finally, I would like to thank the two most important people in the world, James and Darlene Carroll, mom and dad, for giving me this opportunity.

Contents

List of Tables

List of Figures

Chapter 1

INTRODUCTION

The performance of a production well is a function of several variables.

$$Q = f(P_{res}, D_{tubing}, D_{choke}, D_{flowline}, P_{sep}, ...) \tag{1.1}$$

A change in any one of the variables will cause a change in the performance of the well. When designing a new well, or when analyzing an existing well, an engineer will attempt to determine the combination of variables under his or her control that produces the "best" performance of the well. A common procedure to determine the optimal combination of these variables is to develop a model of the well and then use some form of trial and error procedure until the engineer feels that the optimal mix of variables has been determined. In addition to being quite expensive computationally, no certainty can be had that this is the optimal mix of variables as opposed to just a good mix of variables. Fortunately, mathematical techniques are available to determine the optimal mix of these variables without performing a trial and error procedure.

Mathematically, optimization involves finding the extreme values of a function. Given a function of several variables,

$$Z = f(x_1, x_2, x_3, \cdots, x_n) \tag{1.2}$$

an optimization scheme will find the combination of these variables that produces an extreme value in the function, be it a minimum value or a maximum value. There are many examples of optimization. For example, if a function gives an investor's expected return as a function of different investments, numerical optimization of the function will determine the mix of investments that will yield the maximum expected return. This is the basis of modern portfolio theory. If a function gives the difference between a set of data and a model of the data, numerical optimization of the function will produce the best fit of the model to the data. This is the basis for nonlinear parameter estimation. Similar examples can be given for network analysis, queueing theory, decision analysis, etc.

Optimization has historically been used in the petroleum industry to allocate production through pipeline networks, to schedule transoceanic shipments of petroleum

from supply sites to demand sites, to model refinery throughput, and to determine the best use of limited amounts of capital. Lasdon *et al*. (1986) point out that the production sector of the petroleum industry has seen few successful applications of optimization methods.

The objective of this research has been to investigate the effectiveness of nonlinear optimization techniques to optimize the performance of hydrocarbon producing wells. The study consisted of two primary phases: 1) development of a well model that determines well performance, and 2) optimization of well performance with nonlinear optimization techniques.

1.1 Optimization Studies in Petroleum Engineering

Optimization methodologies are the focus of the field of Operations Research, a field that has only been in existence since the 1940's. Operations Research concepts were not adopted by the petroleum industry until the early 1950's. The bulk of the literature since then has been on linear programming techniques applied to reservoir management on a macro-level. For a detailed treatment of optimization methods in petroleum engineering, see Aronofsky (1983).

Aronofsky and Lee (1958) developed a linear programming model to maximize profit by scheduling production from multiple single-well reservoirs. Aronofsky and Williams (1962) extended the same model to investigate the problems of scheduling production for a fixed drilling program and also scheduling drilling for a fixed production schedule. Charnes and Cooper (1961) used linear programming to develop a reservoir model that minimized the cost of wells and facilities subject to a constant production schedule. Attra *et al*. (1961) developed a linear programming model to maximize flow rate subject to several production constraints. All of these models used linear reservoir models based on material balance considerations, and the reservoirs were generally assumed uniform and single phase.

Rowan and Warren (1967) demonstrated how to formulate the reservoir management problem in terms of optimal control theory. Bohannon (1970) used a mixed-integer linear programming model to optimize a pipeline network. O'Dell *et al*. (1973) developed a linear programming model to optimize production scheduling from a multireservoir system. Huppler (1974) developed a dynamic programming model to optimize well and facility design given the delivery schedule and using a material balance

reservoir model. Kuller and Cummings (1974) developed an economic linear programming model of production and investment for petroleum reservoirs.

Several investigators have attempted to couple numerical reservoir simulation with linear programming models. The idea has been to use the reservoir simulator to generate a linearized unit response matrix that could be used with linear programming models. Wattenbarger (1970) developed a linear programming model to schedule production from a gas storage reservoir using this technique. Rosenwald and Green (1974) also used influence functions in a mixed-integer linear programming model that optimized well placement. Murray and Edgar (1979) used influence functions in a mixed-integer linear programming model that optimized well placement and production scheduling. See and Horne (1983), extending on work performed by Coats (1969) and Crichlow (1977), demonstrated how to refine the unit response matrix using nonlinear regression techniques. This work was expanded by Lang and Horne (1983) to consider dynamic programming techniques.

Asheim (1978) studied petroleum developments in the North Sea by coupling reservoir simulation and optimization. Ali *et al*. (1983) used nonlinear programming to study reservoir development and investment policies in Kuwait. McFarland *et al.* (1984) used nonlinear optimization to optimize reservoir production scheduling.

Notice that virtually all of the previous research has attempted to model reservoir performance by linearizing the reservoir performance and feeding this to some variation of linear programming. The main focus in every case was to model the reservoir performance. *None of the models endeavored to optimize the well performance.*

1.2 Modeling Well Performance with Nonlinear Optimization

A clarification of terminology is necessary. In the current literature, the expressions ‘nodal analysis’ and ‘production optimization’ are virtually synonymous. This leads to confusion between nodal analysis and *nonlinear* optimization. A natural question is what distinguishes nonlinear optimization applied to hydrocarbon production systems from the conventional procedure of nodal analysis. The distinction is quite simple: nodal analysis finds the zero of a function which yields the stabilized flow rate of a well (see Figure 1.1); nonlinear optimization finds the zero of the gradient of a function which yields the maximum or minimum value the function can achieve. To restate this important distinction,

nodal analysis finds a solution by locating the zero *of a function*; nonlinear optimization finds the optimum solution by locating the zero *of the gradient* of an objective function.

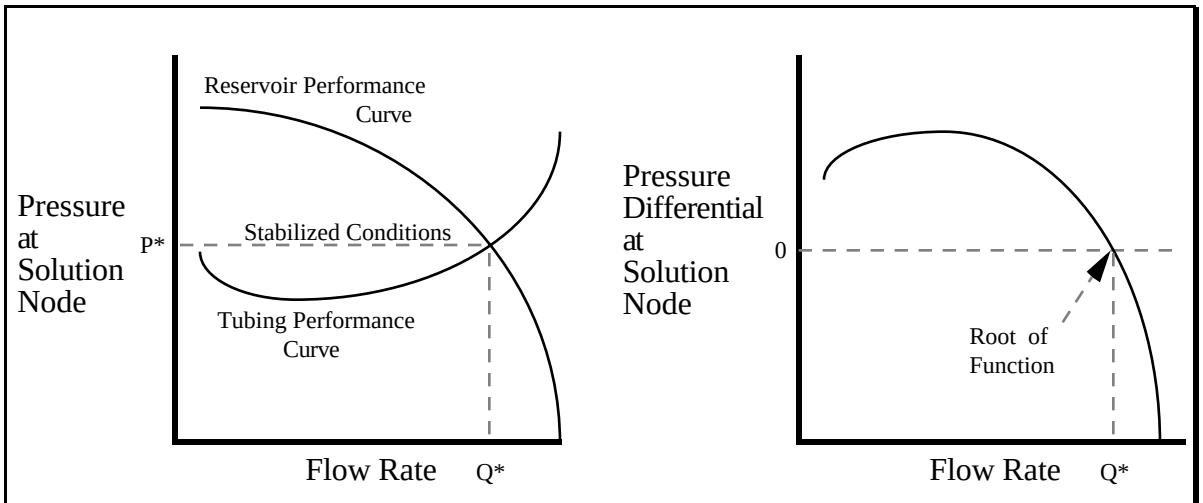

Figure 1.1: Graphical Examples of Nodal Analysis.

The mathematical basis of nodal analysis is relatively straightforward. Several submodels are coupled together to provide a working model of a well (see Figure 1.2). The procedure of nodal analysis is to find the root of the function that causes the pressure differential at the solution node to vanish. This root will be the stabilized flow rate that the well will achieve for the given well conditions. Thus, nodal analysis is not any form of

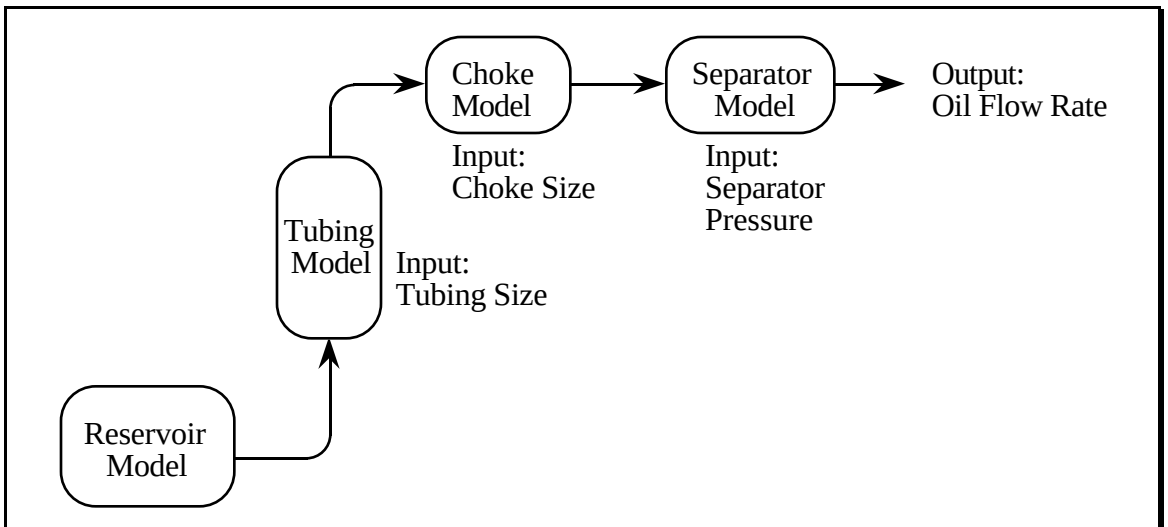

Figure 1.2: Schematic of a Well Model.

optimization, it is merely the procedure of finding the stabilized flow rate that satisfies the function of well performance. The confusion with optimization arises because some people will use nodal analysis in an exhaustive manner to optimize a single variable (e.g., tubing diameter). By holding all other parameters constant, a single parameter is varied to see where the maximum stabilized flow rate will occur. For more information on nodal analysis and 'production systems optimization', see Brown (1977), Chu (1983), Brown and Lea (1985), Golan and Whitson (1986), Lea and Brown (1986), and Hunt (1988).

It is trivial to optimize a function of a single variable: simply plot the variable against the objective criterion and take the extreme value. A single performance curve is all that is required. Matters become complicated if a function of several variables is to be optimized, particularly if the variables are interrelated. To optimize a function of two variables, a performance curve of the first variable plotted against the objective criterion is required for every discrete value of the second variable. The single performance curve required to optimize one variable balloons into a family of performance curves when two variables are optimized. If three variables are optimized, a family of performance curves is required for every discrete value of the third variable. This manner of optimization rapidly becomes intractable because it suffers from the curse of dimensionality--the work involved increases rapidly as additional dimensions are added. This is when the potency of numerical optimization becomes very obvious.

Using nonlinear optimization techniques, there is no limit to the number of decision variables that can be optimized concurrently. All that is required is an objective function that takes all of the decision variables as input and determines the objective variable. Examples of different objective functions are numerous: to maximize the present value of the production stream, to maximize the net present value of the well, to maximize cumulative recovery on an equivalent barrel basis, to minimize the cumulative gas-oil ratio, to minimize the cumulative water-oil ratio, to minimize total investment per equivalent barrel produced, to maximize the rate-of-return of the well, and so on.

As previously mentioned, the study consisted of two primary phases: 1) development of a well model that determines well performance, and 2) optimization of well performance with nonlinear optimization techniques. Chapters 2 through 5 discuss the intricacies involved in the design and development of the various components of the well model as follows: Chapter 2 discusses reservoir material balance and inflow performance, Chapter 3 discusses multiphase flow through vertical tubing, Chapter 4 discusses multiphase flow through surface chokes, and Chapter 5 discusses the separation facilities.

Chapters 6 through 8 discuss the integration of the well model with the nonlinear optimization methods and the conclusions that were drawn. Chapter 6 discusses the theory and implementation of nonlinear optimization techniques. Chapter 7 describes the results of optimizing the well model with various types of nonlinear optimization techniques. Chapter 8 concludes the report by discussing significant findings and proposing ideas for future research.

Chapter 2

RESERVOIR AND INFLOW PERFORMANCE

To replicate the reservoir and inflow performance of a hydrocarbon production system, this study adopted a reservoir model developed by Borthne (1986) at the Norwegian Institute of Technology. The model was originally designed with just this purpose in mind--to provide a simple but functional reservoir component to be included in a larger model. The model provides an accurate representation of constrained reservoir performance that requires minimal computer processing. Since the model was to be used in an optimization study that would require numerous function evaluations, the speed of the model was important.

Borthne's (1986) model is a black-oil model that performs a generalized material balance calculation in concert with an inflow performance relationship based on pseudopressure. The model derives its processing speed from making several simplifying assumptions. Some of the major assumptions are:

- The reservoir is homogeneous, isotropic, horizontal, cylindrical, and of uniform thickness;
- The reservoir is a zero-dimensional single cell that is bounded by no-flow boundaries;
- The reservoir is initially saturated with a single phase fluid--either oil above the bubble point or gas above the dew point--and immobile connate water;
- The reservoir drive mechanism is solution-gas drive for oil and depletion drive for gas;
- The producing gas-oil ratio is constant throughout the reservoir;
- Production occurs under pseudosteady state conditions and at a constant rate;
- Capillary pressure, gravity effects, and coning are negligible.

The reservoir model is constrained by both pressure and flowrate. In addition to specifying a minimum flowing well pressure, two flowrates must be specified: a minimum flowrate and a maximum target flowrate. The model attempts to satisfy the target flowrate without violating the minimum flowing well pressure.

2.1 Reservoir Material Balance

Reproduced here is the theory and procedure of the "generalized" material balance method as implemented in the reservoir model developed by Borthne (1986). For a more exhaustive treatment on the subject, the reader is referred to Borthne's thesis.

For the following discussion, a simple notation scheme is employed. A variable may be given a superscript of S or R, denoting standard conditions or reservoir conditions, respectively. Those without a superscript are implied to be standard conditions. In addition, a variable may be given a two letter subscript, such as OO, OG, GO, or GG. The first letter of the subscript indicates the current phase of the variable and the second letter indicates the source phase of this variable. For example,

$$\rho_{GO}^{S}$$

is the standard density of gas derived from free reservoir oil. Similarly,

$$V_{O}^{R}$$

is the reservoir volume of oil, and

$$Q_{OO}$$

is the standard volumetric flow rate of oil derived from free reservoir oil.

Using this notation scheme, the formation volume factors may be expressed as

$$B_O = \frac{V_O^R}{V_{OO}^S} \tag{2.1}$$

$$B_G = \frac{V_G^R}{V_{GG}^S} \tag{2.2}$$

The solution phase ratios may be expressed as

$$R_S = \frac{V_{GO}^S}{V_{OO}^S} \tag{2.3}$$

$$r_S = \frac{V_{OG}^S}{V_{GG}^S} \tag{2.4}$$

where

R_S is the solution gas-oil ratio

r_S is the solution oil-gas ratio

It should be made clear that the model allows both phases to contain the other phase in solution as shown in Figure 2.1.

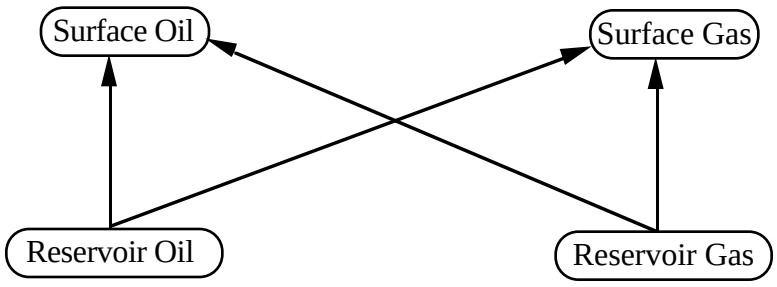

Figure 2.1: Phase Behavior Assumptions of Reservoir Material Balance Procedure.

Though frequently derived in terms of a volumetric balance, conservation of mass provides the basis for the mathematical development of the reservoir material balance. The law of conservation of mass for flow in porous media is

$$\frac{\partial m}{\partial t} + \tilde{q} = -\nabla . \left(\frac{k \rho \nabla P}{\mu} \right) V_B \tag{2.5}$$

where

$\frac{\partial m}{\partial t}$ is the accumulation of mass in the reservoir

$\tilde{q}$ is the mass production rate from the reservoir, the source-sink term, and

$\nabla . \left(\frac{k \rho \nabla P}{\mu} \right) V_B$ is the mass flux term across the reservoir boundaries.

A material balance considers the reservoir to be a single cell with no-flow boundaries. Therefore the mass flux term is zero and the equation simplifies to

$$\frac{\partial m}{\partial t} + \tilde{q} = 0 \tag{2.6}$$

Discretizing and multiplying by a time interval Δt yields

$$\Delta m + \tilde{q} \, \Delta t = 0 \tag{2.7}$$

which simply states that the change of fluid mass in the reservoir must be equivalent to the mass of fluid that was produced or injected.

Equation 2.7 consists of a mass accumulation term and mass source-sink term. The accumulation term consists of the change in the mass of the reservoir fluids over time. The fluid mass in the reservoir at any given time (implied standard conditions) may be given as

$$m_O = m_{OO} + m_{OG} \tag{2.8}$$

$$m_G = m_{GG} + m_{GO}$$

where

$$m_{OO} = \frac{\phi \, S_O \, \rho_{OO}^S}{B_O} V_B \tag{2.9}$$

$$m_{OG} = \frac{\phi \, S_G \, \rho_{OG}^S}{B_G} V_B \tag{2.10}$$

$$m_{GG} = \frac{\phi \, S_G \, \rho_{GG}^S}{B_G} V_B \tag{2.11}$$

$$m_{GO} = \frac{\phi \, S_O \, \rho_{GO}^S}{B_O} V_B \tag{2.12}$$

The source-sink term of Equation 2.7 consists of flowrate terms. These flowrates, defined for the production of oil and gas, are

$$\tilde{q}_O = \tilde{q}_{OO} + \tilde{q}_{OG} \tag{2.13}$$

$$\tilde{q}_G = \tilde{q}_{GG} + \tilde{q}_{GO} \tag{2.14}$$

where

$$\tilde{q}_{OO} = q_{OO}\, \rho_{OO}^{S} \tag{2.15}$$

$$\tilde{q}_{OG} = q_{GG}\, r_S\, \rho_{OG}^{S} \tag{2.16}$$

$$\tilde{q}_{GG} = q_{GG}\, \rho_{GG}^{S} \tag{2.17}$$

$$\tilde{q}_{GO} = q_{OO}\, R_S\, \rho_{GO}^{S} \tag{2.18}$$

Now we introduce a new superscript, the double quotation mark ("). This superscript means that the variable has been normalized to the reservoir bulk volume (i.e. $X'' = X / V_B$), thus making the variable dimensionless. Substituting the mass terms and the source-sink terms back into Equation 2.7 results in four mass-balance equations for oil from oil, oil from gas, gas from gas, and gas from oil:

$$\Delta\left(\frac{\phi\, S_O\, \rho_{OO}^{S}}{B_O}\right) + q''_{OO}\, \rho_{OO}^{S}\, \Delta t = 0 \tag{2.19}$$

$$\Delta\left(\frac{\phi\, S_G\, r_S\, \rho_{OG}^{S}}{B_G}\right) + q''_{GG}\, r_S\, \rho_{OG}^{S}\, \Delta t = 0 \tag{2.20}$$

$$\Delta\left(\frac{\phi\, S_G\, \rho_{GG}^{S}}{B_G}\right) + q''_{GG}\, \rho_{GG}^{S}\, \Delta t = 0 \tag{2.21}$$

$$\Delta\left(\frac{\phi\, S_O\, R_S\, \rho_{GO}^{S}}{B_O}\right) + q''_{OO}\, R_S\, \rho_{GO}^{S}\, \Delta t = 0 \tag{2.22}$$

Combining and simplifying yields two expressions for standard oil and gas production:

$$\Delta\left[\phi\left(\frac{S_O}{B_O} + \frac{S_G\, r_S}{B_G}\,\frac{\rho_{OG}^{S}}{\rho_{OO}^{S}}\right)\right] + q''_{OO}\, \Delta t + q''_{GG}\, \Delta t\, r_S\, \frac{\rho_{OG}^{S}}{\rho_{OO}^{S}} = 0 \tag{2.23}$$

$$\Delta\left[\phi\left(\frac{S_G}{B_G} + \frac{S_O\, R_S}{B_O}\,\frac{\rho_{GO}^{S}}{\rho_{GG}^{S}}\right)\right] + q''_{GG}\, \Delta t + q''_{OO}\, \Delta t\, R_S\, \frac{\rho_{GO}^{S}}{\rho_{GG}^{S}} = 0 \tag{2.24}$$

The volumetric flowrates of both free reservoir oil and free reservoir gas are present in these equations. These may be related to each other by Darcy's law for flow in porous media

$$q_\alpha = \frac{A\ k\ k_{R\alpha}}{\mu_\alpha} \nabla P \tag{2.25}$$

as

$$q''_{OO}\ B_O = C_1 \frac{k_{RO}}{\mu_O} \tag{2.26}$$

$$q''_{GG}\ B_G = C_2 \frac{k_{RG}}{\mu_G} \tag{2.27}$$

where C_1 and C_2 are constants. Capillary pressure is assumed to be zero, so $C_1 = C_2$ and

$$\frac{q''_{OO}\ B_O\ \mu_O}{k_{RO}} = \frac{q''_{GG}\ B_G\ \mu_G}{k_{RG}} \tag{2.28}$$

which, expressed as a gas-oil ratio, is

$$\frac{q''_{GG}}{q''_{OO}} = \frac{k_{RG}\ B_O\ \mu_O}{k_{RO}\ B_G\ \mu_G} \tag{2.29}$$

Multiplying by the time step Δt results in

$$\frac{\Delta G''_{GG}}{\Delta N''_{OO}} = \frac{k_{RG}\ B_O\ \mu_O}{k_{RO}\ B_G\ \mu_G} \tag{2.30}$$

where $\Delta G''_{GG}$ is the incremental gas production from free reservoir gas for time step Δt and $\Delta N''_{OO}$ is the incremental oil production from free reservoir oil for time step Δt expressed as

$$\Delta G''_{GG} = q''_{GG}\ \Delta t \tag{2.31}$$

$$\Delta N''_{OO} = q''_{OO}\ \Delta t \tag{2.32}$$

Substituting these three expressions back into Equations 2.23 and 2.24 gives

$$\Delta\left[\phi\left(\frac{S_O}{B_O} + \frac{S_G\ r_S}{B_G}\frac{\rho^S_{OG}}{\rho^S_{OO}}\right)\right] + \Delta N''_{OO}\left(1 + r_S \frac{\rho^S_{OG}}{\rho^S_{OO}}\frac{k_{RG}\ \mu_O\ B_O}{k_{RO}\ \mu_G\ B_G}\right) = 0 \tag{2.33}$$

$$\Delta\left[\phi\left(\frac{S_G}{B_G}+\frac{S_O\,R_S}{B_O}\frac{\rho^S_{GO}}{\rho^S_{GG}}\right)\right]+\Delta N''_{OO}\left(\frac{k_{RG}\,\mu_O\,B_O}{k_{RO}\,\mu_G\,B_G}+R_S\frac{\rho^S_{GO}}{\rho^S_{GG}}\right)=0 \tag{2.34}$$

These two equations are the oil material balance equation and the gas material balance equation. Notice that they are both written in terms of the incremental oil production, $\Delta N''_{OO}$. These two equations may be abbreviated with the following definitions:

$$\rho^*_O \equiv \frac{\rho^S_{OG}}{\rho^S_{OO}} \tag{2.35}$$

$$\rho^*_G \equiv \frac{\rho^S_{GO}}{\rho^S_{GG}} \tag{2.36}$$

and at time K

$$AO_K \equiv \phi\left(\frac{S_O}{B_O}+\frac{S_G\,r_S\,\rho^*_O}{B_G}\right) \tag{2.37}$$

$$AG_K \equiv \phi\left(\frac{S_G}{B_G}+\frac{S_O\,R_S\,\rho^*_G}{B_O}\right) \tag{2.38}$$

$$RO_K \equiv \left(1+\frac{r_S\,\rho^*_O\,k_{RG}\,\mu_O\,B_O}{k_{RO}\,\mu_G\,B_G}\right) \tag{2.39}$$

$$RG_K \equiv \left(R_S\,\rho^*_G+\frac{k_{RG}\,\mu_O\,B_O}{k_{RO}\,\mu_G\,B_G}\right) \tag{2.40}$$

Substituting these definitions into Equations 2.33 and 2.34 yields the expressions

$$AO_K - AO_{K-1} + \Delta N''_{OO}\,RO_{AVG} = 0 \tag{2.41}$$

$$AG_K - AG_{K-1} + \Delta N''_{OO}\,RG_{AVG} = 0 \tag{2.42}$$

The terms AO and AG represent reservoir conditions at the beginning and end of the time step, specifically at times t_{K-1} and t_K, whereas RO and RG represent the average properties over the time step. Ideally, we would like to evaluate an expression such as

$$RO_{AVG} = \frac{1}{\Delta t}\int_t^{t+\Delta t} RO(P)\,\frac{\partial P}{\partial t}\,dt \tag{2.43}$$

but the estimation of this term would be impractical. Instead, we use arithmetic averages

$$RO_{AVG} = \left(\frac{RO_K + RO_{K-1}}{2}\right) \tag{2.44}$$

$$RG_{AVG} = \left(\frac{RG_K + RG_{K-1}}{2}\right) \tag{2.45}$$

Once we have solved for $\Delta N''_{OO}$, we can solve for the total incremental oil and gas production for the time step as

$$\Delta N''_P = \Delta N''_{OO}\, RO_{AVG} \tag{2.46}$$

$$\Delta G''_P = \Delta N''_{OO}\, RG_{AVG} \tag{2.47}$$

Substituting Equations 2.46 and 2.47 into Equations 2.41 and 2.42 yields

$$AO_K - AO_{K-1} + \Delta N''_P = 0 \tag{2.48}$$

$$AG_K - AG_{K-1} + \Delta G''_P = 0 \tag{2.49}$$

Thus, the material balance errors for the oil and gas material balance equations may be expressed as

$$\Delta E_O = AO_K - AO_{K-1} + \Delta N''_P \tag{2.50}$$

$$\Delta E_G = AG_K - AG_{K-1} + \Delta G''_P \tag{2.51}$$

The solution procedure for the generalized material balance method when the preferred phase is oil is as follows:

1. Specify the constant oil rate, q''_O, and the time step length, Δt.

2. Determine the total incremental oil production, $\Delta N''_P$.

$$\Delta N''_P = q''_O\, \Delta t$$

3. Estimate the average reservoir pressure at the end of the time step. Use this in conjunction with the known average reservoir pressure at the beginning of the time step to determine the average reservoir pressure over the length of time step.

$$P_R = \left(\frac{P_R^K + P_R^{K-1}}{2} \right)$$

Use this average reservoir pressure to determine the pressure dependent properties B_O, B_G, R_S, r_S, μ_O, μ_G, ρ_O^*, ρ_G^*, and ϕ.

4. Calculate oil saturation, S_O, from Equation 2.41 which may be rewritten as

$$\left[\phi \left(\frac{S_O}{B_O} + \frac{(1 - S_W - S_O)\, r_S\, \rho_O^*}{B_G} \right) \right]_K - AO_{K-1} + \Delta N_P'' = 0$$

Since AO_{K-1} was calculated at the last time step, S_O is the only unknown.

5. Calculate the gas saturation

$$S_G = 1 - S_O - S_W$$

6. Calculate the relative permeability ratio as a function of gas saturation. This is done by linear interpolation of $\log(k_{RG} / k_{RO})$ versus S_G. If k_{RG} or k_{RO} is zero, the logarithm is approximated by a large negative or positive number, respectively.

7. Calculate the terms AO_K, AG_K, RO_K, and RG_K.

8. Calculate incremental oil production from free reservoir oil, $\Delta N_{OO}''$, using the oil material balance (Equation 2.41). The term, $\Delta N_{OO}''$, links the oil material balance (Equation 2.41) with the gas material balance (Equation 2.42).

9. Determine the total incremental oil production, $\Delta N_P''$, and the total incremental gas production, $\Delta G_P''$, from Equations 2.46 and 2.47.

10. Calculate the material balance error, ΔE_G, from the gas material balance equation (Equation 2.42).

$$\Delta E_G = AG_K - AG_{K-1} + \Delta G_P''$$

Since the oil material balance equation was satisfied in step 8, it gives no contribution to the error.

11. Proceed, beginning with step 3, until the material balance error converges to within a specified tolerance.

2.2 Reservoir Inflow Performance

The purpose of the reservoir inflow performance component is to relate the average reservoir pressure to the bottomhole flowing pressure according to the flowrate. Once again, for a more exhaustive treatment on the theory and procedure of the inflow performance as implemented in this model, the reader is referred to Borthne's thesis (1986).

Darcy's law provides the fundamental relationship between the average reservoir pressure, the flowing well pressure, and the production rate. For radial flow, Darcy's law is

$$\frac{q_O B_O}{2 \pi r h} = \frac{k k_{RO}}{\mu_O} \frac{\partial P}{\partial r} \tag{2.52}$$

Integrating from the wellbore radius to the radius of drainage

$$\int_{r_w}^{r_e} \frac{q_O B_O}{2 \pi r h} dr = \int_{r_w}^{r_e} \frac{k k_{RO}}{\mu_O} \frac{\partial P}{\partial r} dr \tag{2.53}$$

yields the equation

$$q_o = \frac{2 \pi k h}{\ln (r_e/r_w)} \int_{P_w}^{P_e} \frac{k_{RO}}{\mu_O B_O} dP \tag{2.54}$$

which is valid for steady-state, radial flow, and constant production rate. The expression may be modified for pseudosteady-state flow by the inclusion of a skin term

$$q_o = \frac{2\,\pi\,k\,h}{\ln(r_e/r_w) - 0.75 + S + Dq_o} \int_{P_{wf}}^{P_R} \frac{k_{RO}}{\mu_O\,B_O}\,dP \tag{2.55}$$

Using the concept of pseudopressure, defined as

$$m(P) = \int_0^P \frac{k_{RO}}{\mu_O\,B_O}\,dP \tag{2.56}$$

the above expression may be written as

$$q_o = \frac{2\,\pi\,k\,h}{\ln(r_e/r_w) - 0.75 + S + Dq_o}\left[m(P_R) - m(P_{wf})\right] \tag{2.57}$$

The oil flow rate in this expression refers to the oil flow rate in the reservoir. The flow rate may be converted to a standard flowrate by expanding the pseudopressure integrand to include a term that accounts for oil originating from the reservoir gas.

$$m(P) = \int_0^P \left(\frac{k_{RO}}{\mu_O\,B_O} + \frac{k_{RG}\,r_S}{\mu_G\,B_G}\right) dP \tag{2.58}$$

Notice that for a nonvolatile gas, where the oil-gas ratio, r_S, is zero, the equation reduces to Equation 2.56. The corresponding equation for gas with oil in solution is

$$m(P) = \int_0^P \left(\frac{k_{RG}}{\mu_G\,B_G} + \frac{k_{RO}\,R_S}{\mu_O\,B_O}\right) dP \tag{2.59}$$

We now have a flow equation in terms of modified pseudopressure. The pseudopressure is a function of both pressure and saturation. By assuming a constant producing gas-oil ratio, a relationship may be found between saturation and pressure. In the preceding discussion of the reservoir material balance, the producing gas-oil ratio, R_P, was approximated by

$$R_P = \frac{\Delta G_P}{\Delta N_P} \tag{2.60}$$

Substituting the gas material balance equation for ΔG_P and the oil material balance equation for ΔN_P and defining the mobility ratio as

$$M = \frac{k_{RG}\,\mu_O\,B_O}{k_{RO}\,\mu_G\,B_G} \tag{2.61}$$

Equation 2.60 may be rewritten as

$$R_P = \frac{\Delta N''_{OO}\left(M + R_S\,\rho^*_G\right)}{\Delta N''_{OO}\left(1 + r_S\,\rho^*_O\,M\right)} \tag{2.62}$$

which solving for the mobility ratio yields

$$M = \frac{R_P - R_S\,\rho^*_G}{1 - R_P\,r_S\,\rho^*_O} \tag{2.63}$$

Having calculated the mobility ratio from the material balance equations, we may use the definition of the mobility ratio, Equation 2.61, to determine the relative permeability ratio. Since the relative permeability ratio is a monotonic function of phase saturation, either oil or gas, we may determine phase saturation as a function of pressure for each time step. Subsequently, we may use the phase saturation to determine the individual relative permeability values, k_{RO} and k_{RG}, to be used in the pseudopressure function.

The deliverability expression in its final form, in terms of pseudopressure, is

$$\int_{P_{wf}}^{P_R}\left(\frac{k_{RO}}{\mu_O\,B_O} + \frac{k_{RG}\,r_S}{\mu_G\,B_G}\right)dP = q_o\frac{\ln\left(r_e/r_w\right) - 0.75 + S + Dq_o}{2\,\pi\,k\,h} \tag{2.64}$$

where the right-hand-side of the equation is a constant for each time step. A Newton-Raphson procedure is implemented to find the flowing well pressure that sets the numerical integration of the left-hand-side equal to the constant on the right-hand-side.

Chapter 3

VERTICAL MULTIPHASE FLOW IN TUBING

Multiphase flow is a complex phenomenon that is common in all facets of hydrocarbon production systems. Multiphase flow occurs in the reservoir, in the production string, in the surface pipeline, and throughout the refining process. Typically, an operator will separate the phases at the earliest opportunity to avoid the difficulties associated with flowing multiple phases in the same conduit. However, there are many instances where multiphase flow cannot be eliminated and must be incorporated in the design. For instance, hydrocarbon developments in the deep offshore environment may not have the luxury of immediate separation facilities.

Multiphase flow analysis is used primarily to model the pressure loss that occurs over a segment of conduit. However, it is also used in the design of phase separation facilities to predict liquid slug sizes that the facilities must be able to accommodate.

No completely satisfactory correlations presently exist and, in the view of the extreme complexity of the flow mechanism, it is unlikely there soon will be. Currently, correlations are known to work acceptably under certain sets of conditions and are used accordingly. For a good treatment of two-phase flow correlations, see Brill (1978).

The following is a discussion of the implementation of the multiphase flow component of the well model used for the optimization.

3.1 Principles of Multiphase Flow

The flow of multiphase mixtures is much more difficult to model than single phase-flow. Whereas single-phase flow may be characterized by laminar or turbulent flow, multiphase flow analysis must consider the quantity of the phases, the flow pattern of the phases, the interfacial tension between the phases, stratification between the phases, and the different velocity of the phases. Typically the phases will move at different velocities due to variation in phase densities and viscosities. The disparity in the phase velocities is referred to as the slip velocity. Due to the phases “slipping” past each another, the relative

concentrations of the phases inside the system are distinct from the rates the phases are crossing the system's boundaries. Since the phases are not moving in tandem, the phase volumes inside the system cannot be directly inferred from the phase flowrates. The difference between the *in situ* concentrations inside the system and the concentrations of the phases flowing though the system is known as the holdup phenomenon. Much of the attention of multiphase flow research has been directed at predicting liquid holdup and phase slippage.

Now let us define the primary variables used in multiphase flow analysis. Liquid holdup, H_L, is defined as the volumetric fraction of liquid residing inside the conduit

$$H_L = \frac{\text{Volume of liquid}}{\text{Volume of conduit}} \tag{3.1}$$

This is the true concentration of liquid in the conduit accounting for slippage between the phases. If the boundaries of the system were instantaneously closed and the system were allowed to achieve static equilibrium, this is the fraction of liquid that would settle out. On the contrary, the no-slip liquid holdup, λ_L, assumes no slippage between the phases and therefor the concentration of the phases *in situ* is the same as the fractional flow rates through the system

$$\lambda_L = \frac{Q_L}{Q_L + Q_G} \tag{3.2}$$

Conversely

$$H_G = 1 - H_L \tag{3.3}$$

$$\lambda_G = 1 - \lambda_L \tag{3.4}$$

The slip density and the no-slip density are defined as

$$\rho_S = \rho_L H_L + \rho_G H_G \tag{3.5}$$

$$\rho_{NS} = \rho_L \lambda_L + \rho_G \lambda_G \tag{3.6}$$

Similarly, the slip viscosity and the no-slip viscosity are defined as

$$\mu_S = \mu_L^{H_L} \mu_G^{H_G} \tag{3.7}$$

$$\mu_{NS} = \mu_L \lambda_L + \mu_G \lambda_G \tag{3.8}$$

The superficial velocity of a phase is the velocity the phase would exhibit if it were the only phase in the system and had access to the entire cross-sectional area of the conduit. The superficial velocity for gas and liquid are

$$V_{SG} = \frac{Q_G}{A} \quad \text{and} \quad V_{SL} = \frac{Q_L}{A} \tag{3.9}$$

and the velocity of the mixture is the sum of the superficial velocities

$$V_M = V_{SG} + V_{SL} \tag{3.10}$$

The superficial phase velocities differ from the true velocity of the phases which are

$$V_G = \frac{Q_G}{A\, H_G} \quad \text{and} \quad V_L = \frac{Q_L}{A\, H_L} \tag{3.11}$$

Slip velocity is defined as the difference between the true velocities of the phases.

$$V_S = V_G - V_L \tag{3.12}$$

Most multiphase flow correlations only attempt to model binary systems. In the context of hydrocarbon production, the two phases are typically taken to be gas and liquid. If more than one liquid phase is being considered, such as oil and water, then a weighted average of the liquid parameters is used.

$$\rho_L = \rho_O f_O + \rho_W f_W \tag{3.13}$$

$$\mu_L = \mu_O f_O + \mu_W f_W \tag{3.14}$$

$$\sigma_L = \sigma_O f_O + \sigma_W f_W \tag{3.15}$$

where

$$f_O = \frac{Q_O}{Q_W + Q_O} \tag{3.16}$$

and

$$f_W = \frac{Q_W}{Q_W + Q_O} \tag{3.17}$$

3.2 Derivation of the Mechanical Energy Equation

The theoretical basis of multiphase flow equations is the general energy equation, an expression for the conservation of energy. Simply put, the energy equation requires that the energy of a fluid entering a system, plus any shaft work done on or by the fluid, plus any heat added to or taken from the fluid, plus any change of energy with time in the system, must equal the energy leaving the system. For the energy equation to be practical, it must be expressed in a mechanical form. Govier and Aziz (1972) showed that the mechanical energy equation may be derived from either the momentum equation or the general energy equation. Reproduced here is the derivation from the general energy equation. Starting with a form of the general energy equation for two phases, α and β,

$$d\zeta = \left(M_\alpha + M_\beta\right)\frac{g}{g_C}\,dZ + M_\alpha\,dH_\alpha + M_\beta\,dH_\beta + \frac{M_\alpha\,V_\alpha\,dV_\alpha}{\alpha_\alpha\,g_C} + \frac{M_\beta\,V_\beta\,dV_\beta}{\alpha_\beta\,g_C} \tag{3.18}$$

we must first convert the equation to include only mechanical forms of energy. We do this by substituting, in place of the enthalpy terms, terms involving irreversibilities that account for any degradations of mechanical energy to internal energy. The equation becomes

$$\left(M_\alpha + M_\beta\right)\frac{g}{g_C}\,dZ + \left(M_\alpha\,\upsilon_\alpha + M_\beta\,\upsilon_\beta\right)dP + \frac{M_\alpha\,V_\alpha\,dV_\alpha}{\alpha_\alpha\,g_C} + \frac{M_\beta\,V_\beta\,dV_\beta}{\alpha_\beta\,g_C} + M_\alpha\,d\Phi_\alpha + M_\beta\,d\Phi_\beta = 0 \tag{3.19}$$

Rearranging, the equation becomes

$$-dP = \left(\frac{M_\alpha + M_\beta}{Q_\alpha + Q_\beta}\right)\frac{g}{g_C}\,dZ + \left(\frac{M_\alpha\,V_\alpha\,dV_\alpha}{\alpha_\alpha\,g_C} + \frac{M_\beta\,V_\beta\,dV_\beta}{\alpha_\beta\,g_C}\right)\frac{1}{Q_\alpha + Q_\beta} + \frac{M_\alpha\,d\Phi_\alpha + M_\beta\,d\Phi_\beta}{Q_\alpha + Q_\beta} \tag{3.20}$$

Distinguishing between the irreversibilities that occur in each phase is arbitrary, so we group all of the irreversibility terms into a single term

$$-dP_F = \frac{M_\alpha\,d\Phi_\alpha + M_\beta\,d\Phi_\beta}{Q_\alpha + Q_\beta} \tag{3.21}$$

and the equation becomes

$$-dP = \frac{1}{Q_\alpha + Q_\beta}\left[\left(M_\alpha + M_\beta\right)\frac{g}{g_C}\,dZ + \frac{M_\alpha\, V_\alpha\, dV_\alpha}{\alpha_\alpha\, g_C} + \frac{M_\beta\, V_\beta\, dV_\beta}{\alpha_\beta\, g_C}\right] - dP_F \qquad (3.22)$$

Applying the equation to a finite length of the conduit, inclined at an angle θ from horizontal, and defining $\Delta P = (P_1 - P_2)$, the equation becomes

$$\Delta P = \left(\frac{M_\alpha + M_\beta}{Q_\alpha + Q_\beta}\right)\frac{g}{g_C}\,L\sin\theta + \left[\frac{M_\alpha\left(V_{\alpha 2}^2 - V_{\alpha 1}^2\right)}{2\,\alpha_\alpha\left(Q_\alpha + Q_\beta\right)g_C} + \frac{M_\beta\left(V_{\beta 2}^2 - V_{\beta 1}^2\right)}{2\,\alpha_\beta\left(Q_\alpha + Q_\beta\right)g_C}\right] - dP_F \qquad (3.23)$$

This equation may be expressed as a pressure gradient and generalized to a form consisting of three terms

$$\frac{dP}{dZ} = \left(\frac{dP}{dZ}\right)_{HH} + \left(\frac{dP}{dZ}\right)_{KE} + \left(\frac{dP}{dZ}\right)_F \qquad (3.24)$$

where

$\left(\frac{dP}{dZ}\right)_{HH}$ is the pressure gradient due to hydrostatic head, or potential energy, of the fluid,

$\left(\frac{dP}{dZ}\right)_{KE}$ is the pressure gradient due to the acceleration, or kinetic energy, of the fluid, and

$\left(\frac{dP}{dZ}\right)_F$ is the pressure gradient due to friction.

The impetus of most multiphase flow correlations is to predict the potential energy effect by accurately predicting the liquid holdup. Of secondary interest is how to best predict the two-phase friction effect. The kinetic energy effect, which is usually negligible, has largely been ignored by the research community.

The many empirical correlations that have been developed to model the performance of two-phase flow in conduits may be distinguished in the manner they determine these three components. Correlations may easily be classified by whether the correlation accounts for slippage between the phases and whether the correlation allows for different flow regimes. Many of the earlier correlations assume no slippage between the phases and do not distinguish between different flow regimes. Correlations in this category include Poettmann and Carpenter (1952), Baxendall and Thomas (1961), and Fancher and Brown (1963). Hagedorn and Brown (1965) allow for slippage between the phases but do not

account for different flow regimes. The more recent correlations of Duns & Ros (1963), Orkiszewski (1967), Aziz *et al*. (1972), and Beggs & Brill (1973) account for slippage between the phases and provide different algorithms to model different flow regimes.

3.3 The Correlation of Hagedorn and Brown (1965)

The version of Equation 3.24 presented by Hagedorn and Brown (1965), in field units, is

$$144\,\frac{\Delta P}{\Delta Z} = \overline{\rho}_S + \frac{4\,f_m\,(Q_o + Q_w)^2\,M^2}{2.9652\ \text{x}\ 10^{11}\,D^5\,\overline{\rho}_S} + \frac{\overline{\rho}_S\,\Delta\left(\frac{V_M}{2g_c}\right)}{\Delta Z} \tag{3.25}$$

Hagedorn and Brown (1965) adopted an approach of backing out the liquid holdup. After obtaining multiphase flow performance data from an experimental well, the acceleration term and the friction term were solved in the conventional manner and then a value of liquid holdup was calculated to satisfy the observed pressure gradient. Thus the liquid holdup used in the above equation is not a true measure of the volume of the pipe occupied by the liquid but is merely a correlating parameter.

To correlate the liquid holdup, Hagedorn and Brown (1965) drew upon the dimensionless groups defined by Ros (1961). These are N_{VL}, the liquid velocity number; N_{VG}, the gas velocity number; N_D, the diameter number; and N_L, the liquid viscosity number, modified by Hagedorn and Brown (1965) as

$$N_{LV} = 1.938\ V_{SL}\ \sqrt[4]{\rho_L/\sigma_L} \tag{3.26}$$

$$N_{GV} = 1.938\ V_{SG}\ \sqrt[4]{\rho_L/\sigma_L} \tag{3.27}$$

$$N_D = 120.872\ D\ \sqrt{\rho_L/\sigma_L} \tag{3.28}$$

$$N_L = 0.15726\ \mu_L\ \sqrt[4]{1/\rho_L\sigma_L^3} \tag{3.29}$$

These four numbers are used in conjunction with three graphs published by Hagedorn and Brown in their original paper (1965) to obtain H_L as follows:

- N_L is used with the first graph to obtain the product CN_L, where C is a correlating parameter.

- The term $\frac{N_{GV}\, N_L^{0.38}}{N_D^{2.14}}$ is used with the second graph to obtain ψ, where ψ is a second correlating parameter.
- The term $\left(\frac{N_{LV}}{N_{GV}^{0.575}}\right)\left(\frac{P}{P_{SC}}\right)^{0.1}\left(\frac{CN_L}{N_D}\right)$ is used in association with the third graph to obtain the term $\left(\frac{H_L}{\psi}\right)$ which yields the liquid holdup.

These graphs have been tabulated and are presented in Table 3.1.

Table 3.1: Correlating Functions of Hagedorn and Brown (1965).

GRAPH 1		GRAPH 2		GRAPH 3	
N_L	CN_L	$\frac{N_{GV}\, N_L^{0.38}}{N_D^{2.14}}$	ψ	$\left(\frac{N_{LV}}{N_{GV}^{0.575}}\right)\left(\frac{P}{P_{SC}}\right)^{0.1}\left(\frac{CN_L}{N_D}\right)$	$\left(\frac{H_L}{\psi}\right)$
.002	.0019	.010	1.00	0.2	.04
.005	.0022	.020	1.10	0.5	.09
.010	.0024	.025	1.23	1.	.15
.020	.0028	.030	1.40	2.	.18
.030	.0033	.035	1.53	5.	.25
.060	.0047	.040	1.60	10.	.34
.100	.0064	.045	1.65	20.	.44
.150	.0080	.050	1.68	50.	.65
.200	.0090	.060	1.74	100.	.82
.400	.0115	.070	1.78	200.	.92
---	---	.080	1.80	300.	.96
---	---	.090	1.83	1000.	1.00

Having obtained the correlated value for liquid holdup, the pressure gradient due to hydrostatic head is simply

$$\left(\frac{dP}{dZ}\right)_{HH} = \frac{g}{g_C}\left(\rho_L H_L + \rho_G H_G\right) = \frac{g}{g_C}\rho_S \qquad (3.30)$$

In determining the friction component, Hagedorn and Brown (1965) elected to correlate a two-phase friction factor with a two-phase Reynold's number using the standard Moody diagram. The two-phase Reynold's number, as defined by Hagedorn and Brown (1965), is

$$Re_{HB} = \frac{\rho_{NS}\, V_M\, D}{\mu_S} \tag{3.31}$$

Having obtained the two-phase friction factor from a Moody diagram using the two-phase Reynold's number, the friction component of the total pressure gradient is given by

$$\left(\frac{dP}{dZ}\right)_F = \frac{f_M\, \rho_{NS}^2\, V_M^2}{2\, g_C\, \rho_S D} \tag{3.32}$$

We can account for the acceleration effects of the kinetic energy component by defining E_K as

$$E_K = \frac{V_M\, V_{SG}\, \rho_{NS}}{g_C\, P} \tag{3.33}$$

The total pressure gradient is then given by

$$\frac{dP}{dZ} = \frac{\left(\frac{dP}{dZ}\right)_{HH} + \left(\frac{dP}{dZ}\right)_F}{1 - E_K} \tag{3.34}$$

Treating the acceleration component in this fashion requires caution: as the value of E_K approaches one, the total pressure gradient becomes indeterminant. This is physically analogous to sonic or choked flow and is common for high gas velocities at low pressures. Since numerical instabilities arise as you begin to approach one, the value of E_K is typically constrained below a certain ceiling value. In the model developed for this report, E_K is not allowed to exceed a conservative value of 0.6.

Many people employ a modified version of the Hagedorn and Brown (1965) correlation, the modification being that the Griffith and Wallis (1961) method is used for the bubble flow regime. The Griffith and Wallis (1961) modification is made if

$$\frac{V_{SG}}{V_M} < L_B \tag{3.35}$$

where

$$L_B = 1.071 - \left(\frac{0.2218\, V_M^2}{D}\right) ; \quad L_B \geq 0.13 \tag{3.36}$$

If the bubble flow regime is indicated, then the liquid holdup for bubble flow, as determined by Griffith and Wallis (1961), is given by the expression

$$H_L = 1 - \frac{1}{2}\left[1 + \frac{V_M}{V_S} - \sqrt{\left(1 + \frac{V_M}{V_S}\right)^2 - 4\,\frac{V_{SG}}{V_S}}\,\right] \tag{3.37}$$

where the slip velocity, V_S, is assumed to be constant at 0.8 ft/sec. The density component of the total pressure gradient is determined from the expression

$$\left(\frac{dP}{dZ}\right)_{HH} = \frac{g}{g_C}\,\rho_s = \frac{g}{g_C}\,(\rho_L\,H_L + \rho_G\,H_G) \tag{3.38}$$

The friction component for the bubble flow region is based solely on the liquid phase and is given by

$$\left(\frac{dP}{dZ}\right)_F = \frac{f_M\,\rho_L\left(\frac{V_{SL}}{H_L}\right)^2}{2\,g_C\,D} \tag{3.39}$$

where the Moody friction factor is based on the Reynold's number of the liquid

$$Re = \frac{\rho_L\,V_{SL}\,D}{H_L\,\mu_L} \tag{3.40}$$

The acceleration component was considered to be negligible in the bubble flow regime. Therefore, the pressure gradient in the bubble flow regime is given by

$$\left(\frac{dP}{dZ}\right)_{BUB} = \left(\frac{dP}{dZ}\right)_{HH} + \left(\frac{dP}{dZ}\right)_F \tag{3.41}$$

3.4 The Correlation of Aziz, Govier, and Fogarasi (1972)

Aziz, Govier, and Fogarasi (1972) proposed a multiphase flow correlation that was dependent on the flow regime. The Aziz *et al.* (1972) correlation has some theoretical justification and is considered to be one of the least empirical correlations available. Four flow regimes are considered: Bubble, slug, transition, and annular-mist (see Figure 3.1). Aziz *et al.* (1972) presented original correlations for the bubble and slug flow regimes and used the method of Duns and Ros (1963) for the transition and annular-mist flow regimes. The flow regimes are identified with the following variables:

$$N_X = V_{SG}\left(\frac{\rho_G}{.0764}\right)^{1/3}\left(\frac{72\,\rho_L}{62.4\,\sigma_L}\right)^{1/4} \tag{3.42}$$

$$N_Y = V_{SL} \left(\frac{72\ \rho_L}{62.4\ \sigma_L} \right)^{1/4} \tag{3.43}$$

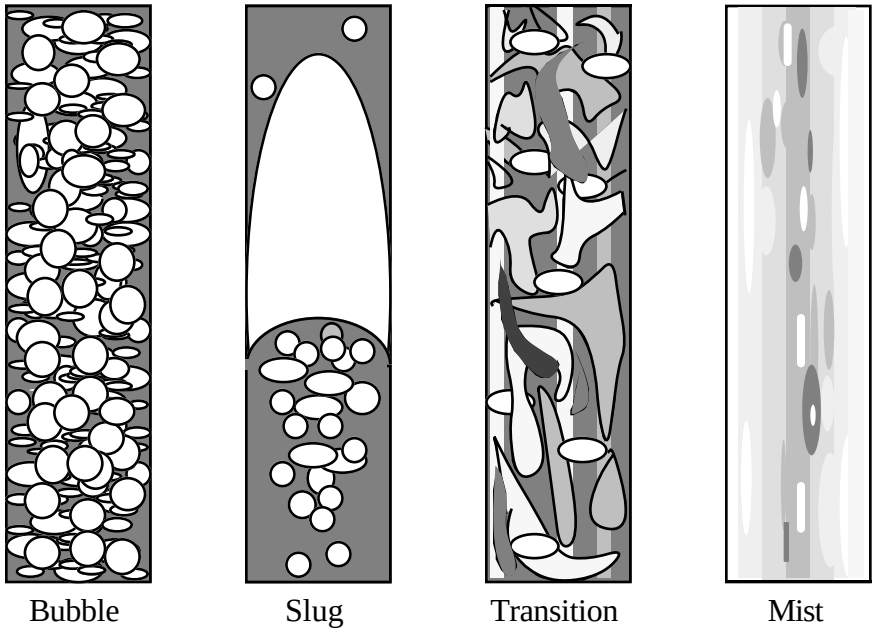

Figure 3.1: Flow Regimes of Aziz, Govier, and Fogarasi (1972).

N_X and N_Y give the location within the flow map while the boundaries of the flow regimes are given by

$$B_{12} = 0.51\ (100\ N_Y)^{0.172} \tag{3.44}$$

$$B_{23} = 8.6 + 3.8\ N_Y \tag{3.45}$$

$$B_{34} = 70\ (100\ N_Y)^{-0.152} \tag{3.46}$$

The flow regimes may be identified as follows:

Bubble Flow: $N_X < B_{12}$ (3.47)

Slug Flow: $B_{12} \le N_X < B_{23}$ (3.48)

Transition Flow: $B_{23} \le N_X < B_{34}$; $N_Y < 4$ (3.49)

Annular-Mist: $B_{34} \le N_X$ (3.50)

The Aziz *et al.* (1972) flow map is presented in Figure 3.2.

A paper by Hazim and Nimat (1989) proposed that the performance of the Aziz *et al.* (1972) correlation could be improved by using other flow-pattern maps instead of the map proposed by Aziz *et al.* (1972). For their specific data set, best performance was attained when the Aziz *et al.* (1972) correlation was used in conjunction with the Duns and Ros (1963) flow-pattern map.

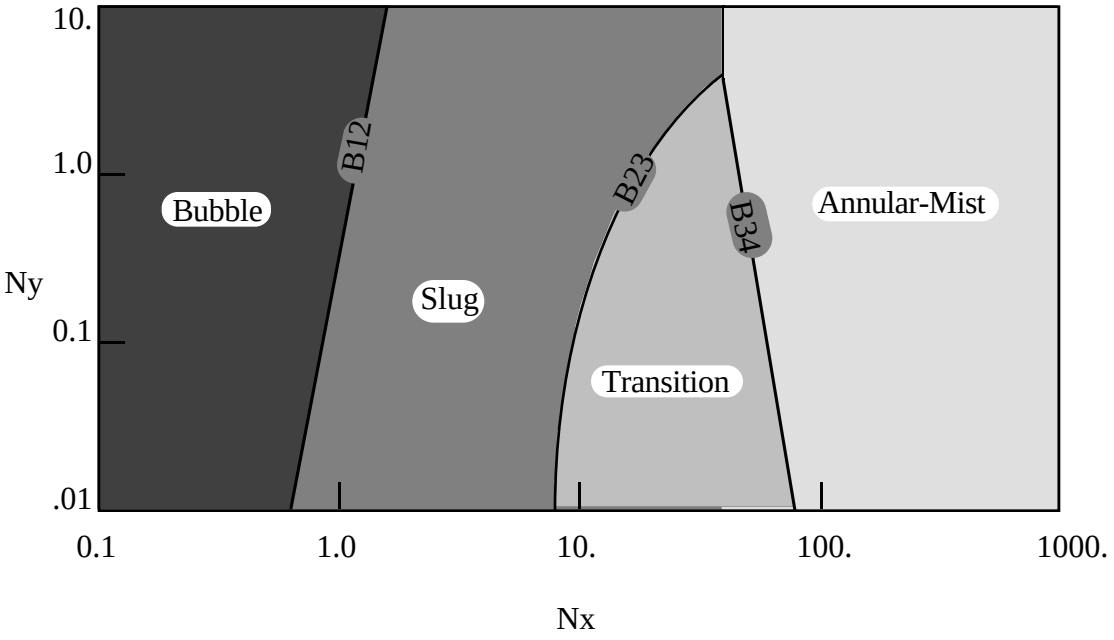

Figure 3.2: Flow-Pattern Map Proposed by Aziz, Govier, and Fogarasi (1972).

3.4.1 Bubble Flow Regime

To obtain the pressure gradient due to fluid density in the bubble flow regime, Aziz *et al.* (1972) proposed to define the liquid holdup as

$$H_L = 1 - \frac{V_{SG}}{V_{BF}} \tag{3.51}$$

where the absolute bubble rise velocity is

$$V_{BF} = 1.2\, V_M + V_{BS} \tag{3.52}$$

and the bubble rise velocity is

$$V_{BS} = 1.41 \left(\frac{\sigma_L\, g\, (\rho_L - \rho_G)}{\rho_L^2} \right)^{1/4} \tag{3.53}$$

The hydrostatic head component of the total pressure gradient is then

$$\left(\frac{dP}{dZ}\right)_{HH} = \frac{g}{g_C}\left(\rho_L H_L + \rho_G H_G\right) = \frac{g}{g_C}\rho_S \tag{3.54}$$

To determine the friction component, they proposed to use

$$\left(\frac{dP}{dZ}\right)_F = \frac{f_M \rho_S V_M^2}{2 g_C D} \tag{3.55}$$

where the Moody friction factor is obtained using a Reynold's number of

$$Re = \frac{\rho_L V_M D}{\mu_L} \tag{3.56}$$

The acceleration component was considered to be negligible in the bubble flow regime. Therefore, the total pressure gradient for the bubble flow regime is given by

$$\left(\frac{dP}{dZ}\right)_{BUB} = \left(\frac{dP}{dZ}\right)_{HH} + \left(\frac{dP}{dZ}\right)_F \tag{3.57}$$

3.4.2 Slug Flow Regime

The density component in the slug flow regime uses the same definition for liquid holdup and V_{BF} employed in the bubble flow regime. However, V_{BS} is defined as

$$V_{BS} = C\left(\frac{g D (\rho_L - \rho_G)}{\rho_L}\right)^{1/2} \tag{3.58}$$

where

$$C = 0.345\left[1 - \exp(-0.029\, N_V)\right]\left[1 - \exp\left(\frac{3.37 - N_E}{m}\right)\right] \tag{3.59}$$

$$N_E = \frac{g D (\rho_L - \rho_G)}{\sigma_L} \tag{3.60}$$

$$N_V = \frac{\left(g D^3 \rho_L (\rho_L - \rho_G)\right)^{1/2}}{\mu_L} \tag{3.61}$$

where m in Equation 3.59 is evaluated as follows:

N_V	m

$N_V \leq 18$	25
$18 < N_V < 250$	$69\ N_V^{-0.35}$
$250 \leq N_V$	10

(3.62)

(3.63)

(3.64)

Having obtained the liquid holdup, the hydrostatic head component of the total pressure gradient is

$$\left(\frac{dP}{dZ}\right)_{HH} = \frac{g}{g_C}\left(\rho_L H_L + \rho_G H_G\right) = \frac{g}{g_C}\rho_S \tag{3.65}$$

The friction component in slug flow is evaluated as

$$\left(\frac{dP}{dZ}\right)_F = \frac{f_M \rho_L H_L V_M^2}{2 g_C D} \tag{3.66}$$

where the Moody friction is obtained using a Reynold's number of

$$Re = \frac{\rho_L V_M D}{\mu_L} \tag{3.67}$$

As in the bubble flow regime, the acceleration component was considered to be negligible in the slug flow regime. Therefore, the total pressure gradient for the slug flow regime is given by

$$\left(\frac{dP}{dZ}\right)_{SLUG} = \left(\frac{dP}{dZ}\right)_{HH} + \left(\frac{dP}{dZ}\right)_F \tag{3.68}$$

3.4.3 Transition Flow Regime

The transition flow region is, as the name indicates, a region of transition between the slug flow region and the annular-mist flow region. When flow occurs within the transition region, the pressure gradient is obtained by performing a linear interpolation between the slug and annular-mist regions, as suggested by Duns and Ros (1963). The interpolation is performed as follows:

$$\left(\frac{dP}{dZ}\right)_{TRANS} = \left(\frac{N_3 - N_X}{N_3 - N_2}\right)\left(\frac{dP}{dZ}\right)_{SLUG} + \left(\frac{N_X - N_2}{N_3 - N_2}\right)\left(\frac{dP}{dZ}\right)_{MIST} \tag{3.69}$$

3.4.4 Annular-Mist Flow Regime

For modeling the annular-mist flow regime, Aziz *et al.* (1972) used the procedure developed by Duns and Ros (1963). Duns and Ros assumed that the high gas velocity of the annular-mist region would allow no slippage to occur between the phases. The mixture density used to calculate the density component is, therefore, the no-slip density, ρ_{NS}. The expression for the density component is

$$\left(\frac{dP}{dZ}\right)_{HH} = \frac{g}{g_C}\rho_{NS} = \frac{g}{g_C}\left(\rho_L \lambda_L + \rho_G \lambda_G\right) \tag{3.70}$$

The friction component for the annular-mist region is based solely on the gas phase and is given by

$$\left(\frac{dP}{dZ}\right)_F = \frac{f_M \rho_G V_{SG}^2}{2 g_C D} \tag{3.71}$$

where the Moody friction factor is based on the Reynold's number of the gas

$$Re = \frac{\rho_G V_{SG} D}{\mu_G} \tag{3.72}$$

Duns and Ros (1963) gave special treatment to the manner that the relative roughness was determined. They discovered that the pipe roughness was altered by the thin layer of liquid on the wall of the pipe. Two variables are used to characterize this effect. The first is a form of the Weber number

$$N_{WE} = \frac{\rho_G V_{SG}^2 \varepsilon}{\sigma_L} \tag{3.73}$$

and the second is dimensionless number based on liquid viscosity

$$N_\mu = \frac{\mu_L}{\rho_L \sigma_L \varepsilon} \tag{3.74}$$

Duns and Ros (1963) proposed the following relationship to model the relative roughness:

$N_{WE} N_\mu \le 0.005$	$\frac{\varepsilon}{D} = \frac{0.0749 \sigma_L}{\rho_G V_{SG}^2 D}$

(3.75)

$N_{WE}\, N_{\mu} > 0.005$	$\frac{\varepsilon}{D} = \frac{0.3713\, \sigma_L}{\rho_G\, V_{SG}^2\, D} \left(N_{WE}\, N_{\mu}\right)^{0.302}$

(3.76)

The value of the relative roughness is constrained to be no less than the actual relative roughness of the pipe and no more than 0.5.

For values of relative roughness greater than 0.05, the limits of the Moody diagram are approached. Duns and Ros (1963) proposed the following relation for the moody friction factor for values of relative roughness greater than 0.05:

$$f_M = 4\left[\frac{1}{\left(4 \log\left(0.27\, \frac{\varepsilon}{D}\right)\right)^2} + 0.067 \left(\frac{\varepsilon}{D}\right)^{1.73}\right] \tag{3.77}$$

We can account for the acceleration component by defining E_K as

$$E_K = \frac{V_M\, V_{SG}\, \rho_{NS}}{g_C\, P} \tag{3.78}$$

The total pressure gradient is then given by

$$\left(\frac{dP}{dZ}\right)_{MIST} = \frac{\left(\frac{dP}{dZ}\right)_{HH} + \left(\frac{dP}{dZ}\right)_F}{1 - E_K} \tag{3.79}$$

As mentioned earlier, treating the kinetic energy term in this fashion requires care as the term will become indeterminant as E_K approaches one.

3.5 The Correlation of Orkiszewski (1967):

The work of Orkiszewski (1967) is a composite product: after testing the available correlations for their accuracy, he selected the flow correlations he considered to be the most accurate. These include the Griffith and Wallis (1961) method for bubble flow, the Duns and Ros (1963) method for annular-mist flow and transition flow, and a method he proposed for slug flow. The Griffith and Wallis (1961) method was previously discussed with the Hagedorn and Brown (1965) correlation and the Duns and Ros (1963) method was previously discussed with the Aziz *et al.* (1972) correlation. Discussion of these methods will not be repeated here.

Orkiszewski's contribution was an original correlation to model slug flow. The flow map of Orkiszewski (1967) is partitioned by the boundaries of

$$L_B = 1.071 - \left(\frac{0.2218\ V_M^2}{D}\right) ; \quad L_B \geq 0.13 \tag{3.80}$$

$$L_S = 50 + 36\ N_{LV} \tag{3.81}$$

$$L_M = 75 + 84\ N_{LV}^{0.75} \tag{3.82}$$

where the dimensionless numbers N_{LV} and N_{GV}, as proposed by Ros (1961), are

$$N_{LV} = V_{SL} \sqrt[4]{\frac{\rho_L}{g\,\sigma}} \tag{3.83}$$

$$N_{GV} = V_{SG} \sqrt[4]{\frac{\rho_L}{g\,\sigma}} \tag{3.84}$$

The flow regimes are identified by the following rules:

Bubble	$\frac{V_{SG}}{V_M} < L_B$
Slug	$\frac{V_{SG}}{V_M} > L_B$ and $N_{GV} < L_S$
Transition	$L_S < N_{GV} < L_M$
Annular-Mist	$L_M < N_{GV}$

The flow-pattern map suggested by Orkiszewski (1967) is shown in Figure 3.3.

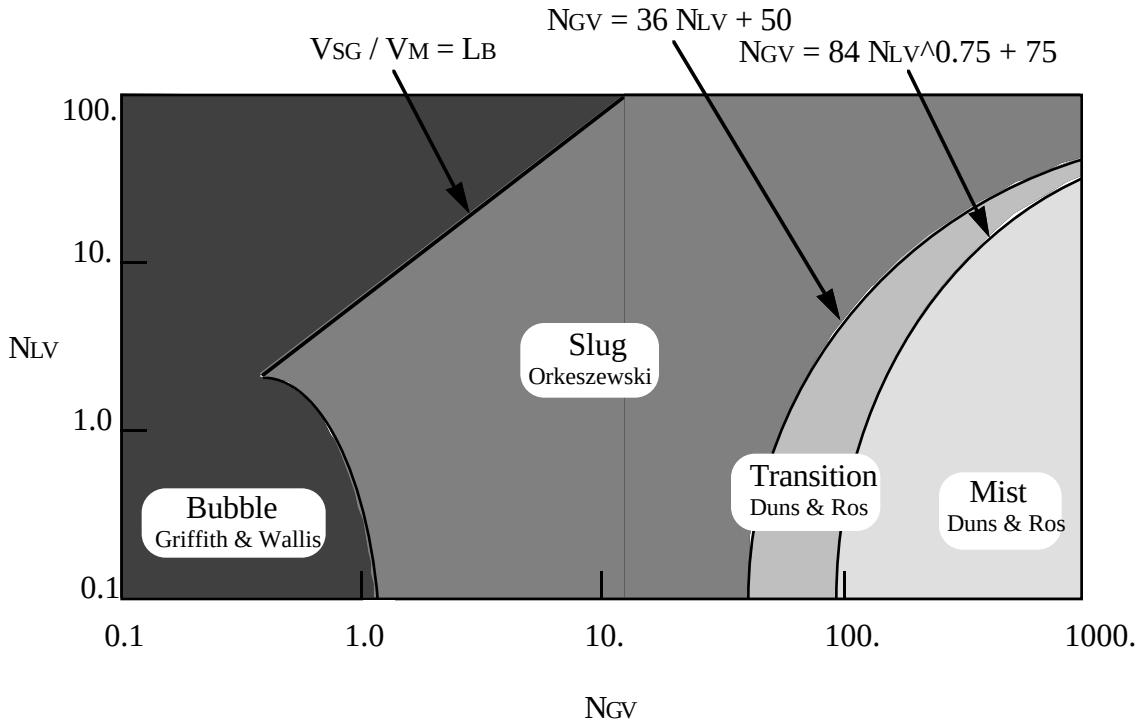

Figure 3.3: Flow-Pattern Map Proposed by Orkiszewski (1967).

To model the slug flow regime, Orkiszewski (1967) defined two-phase density as

$$\rho_S = \frac{\rho_L \left(V_{SL} + V_B \right) + \rho_G V_{SG}}{V_M + V_B} + \rho_L \delta \tag{3.85}$$

Two different Reynold's numbers are required to find V_B

$$N_{RE_B} = \frac{\rho_L V_B D}{\mu_L} \tag{3.86}$$

$$N_{RE_L} = \frac{\rho_L V_M D}{\mu_L} \tag{3.87}$$

The procedure to find V_B is iterative:

1. Estimate V_B. Orkiszewski (1967) recommends $V_B = 0.5 \sqrt{g D}$.
2. Calculate N_{RE_B} using the value of V_B from step 1.
3. Calculate V_B according to the following rule set.
4. Repeat until convergence is achieved.

The rule-set to evaluate V_B is

$N_{RE_B} \le 3000$	$V_B = \left(0.546 + 8.74\text{x}10^{-6}\, N_{RE_L}\right)\sqrt{g\,D}$	(3.88)
$3000 < N_{RE_B} < 8000$	$\xi = \left(0.251 + 8.7\text{x}10^{-6}\, N_{RE_L}\right)\sqrt{g\,D}$ $V_B = \frac{1}{2}\left[\xi + \sqrt{\xi^2 + \frac{13.59\,\mu_L}{\rho_L\sqrt{D}}}\right]$	(3.89)
$8000 \le N_{RE_B}$	$V_B = \left(0.35 + 8.74\text{x}10^{-6}\, N_{RE_L}\right)\sqrt{g\,D}$	(3.90)

The variable δ in the two-phase density expression is given by

WOR	V_M	δ	
> 3	< 10	$\frac{(0.013 \log \mu_L)}{D^{1.38}} - 0.681 + 0.232 \log V_M - 0.428 \log D$	(3.91)
> 3	> 10	$\frac{(0.045 \log \mu_L)}{D^{0.799}} - 0.709 - 0.162 \log V_M - 0.888 \log D$	(3.92)
< 3	< 10	$\frac{0.0127 \log(\mu_L + 1)}{D^{1.415}} - 0.284 + 0.167 \log V_M - 0.113 \log D$	(3.93)
< 3	> 10	$\frac{0.0274 \log(\mu_L + 1)}{D^{1.371}} + 0.161 + 0.569 \log D$ $-\log V_M\left[\left(\frac{0.01 \log(\mu_L + 1)}{D^{1.571}}\right) + 0.397 + 0.63 \log D\right]$	(3.94)

where the value of δ is constrained by

$V_M < 10$	$\delta \geq -0.065\ V_M$ (3.95)
$V_M > 10$	$\delta \geq \frac{-V_B}{V_M + V_B}\left(1 - \frac{\rho_S}{\rho_L}\right)$ (3.96)

Having obtained the two-phase density, the density component of the total pressure gradient is

$$\left(\frac{dP}{dZ}\right)_{HH} = \frac{g}{g_C}\rho_s = \frac{g}{g_C}(\rho_L H_L + \rho_G H_G) \tag{3.97}$$

The friction component is given by

$$\left(\frac{dP}{dZ}\right)_F = \frac{f_M \rho_L V_M^2}{2 g_C D}\left[\left(\frac{V_{SL} + V_B}{V_M + V_B}\right) + \delta\right] \tag{3.98}$$

where the Moody friction factor is based on the Reynold's number

$$Re = \frac{\rho_L V_M D}{\mu_L} \tag{3.99}$$

The acceleration component was considered negligible for the slug flow regime. Therefore, the total pressure gradient for the slug flow regime is given by

$$\left(\frac{dP}{dZ}\right)_{SLUG} = \left(\frac{dP}{dZ}\right)_{HH} + \left(\frac{dP}{dZ}\right)_F \tag{3.100}$$

3.6 Implementing the Correlations

Implementing the empirical multiphase flow correlations can be difficult due to the codependency of the pressure and the fluid properties. Because the fluid properties and the pressure are mutually dependent--it takes fluid properties to determine the pressure and conversely it takes pressure to determine the fluid properties--the procedure is iterative and must be performed for small increments over which the pressure and fluid properties may be assumed constant. Thus the length of the conduit is traversed in small increments, determining a new pressure at each step, in what is known as a pressure traverse.

Although a pressure traverse may be performed by iterating on either length or on pressure, iterating on pressure is the preferred method. By iterating on pressure, the sum of the length intervals can be set to equal the length of the conduit and no interpolation is required in the final step. Moreover, the scheme of iterating on length can have numerical difficulties associated with downward flow due to the friction component and the density component working against each other. The general procedure of performing the pressure traverse is detailed in Figure 3.4.

Gregory *et al*. (1980) demonstrated that the pressure traverse is direction dependent. They concluded that significantly higher accuracy is achieved when the pressure traverse proceeds from the high pressure region (bottomhole) to the low pressure region (wellhead).

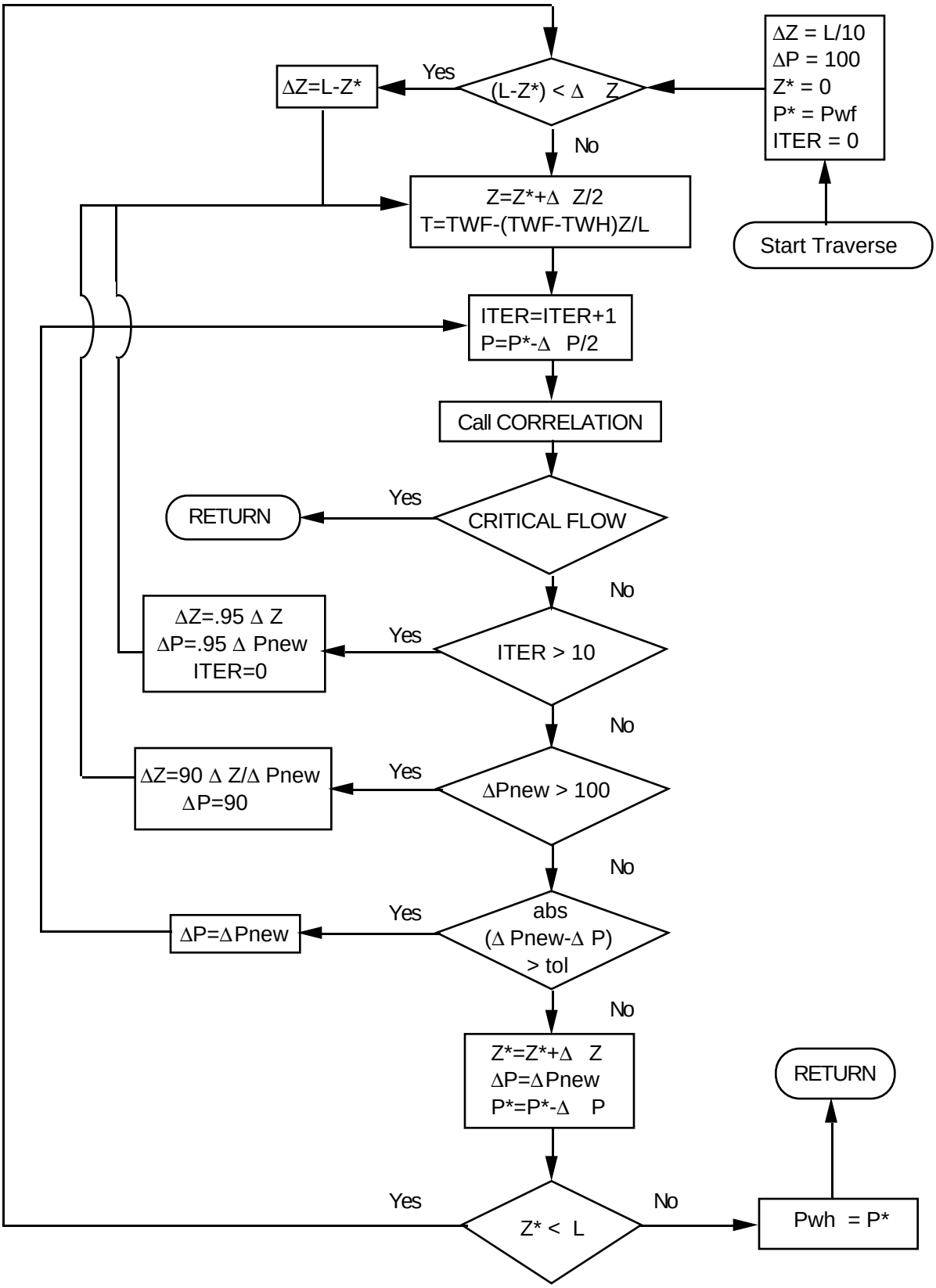

Figure 3.4: Pressure Traverse Flow Diagram.

Chapter 4

SURFACE CHOKES

Virtually all flowing wells utilize some form of surface restriction to regulate the flowrate. Typically, a surface choke is located immediately following the wellhead. For offshore wells, the "storm" choke is located upstream of the wellhead beneath the mudline. There are two general types of chokes: positive chokes and adjustable chokes. An illustration of a positive choke is shown in Figure 4.1.

The reasons for having a choking device in the production system are to

- protect reservoir and surface equipment from pressure fluctuations;

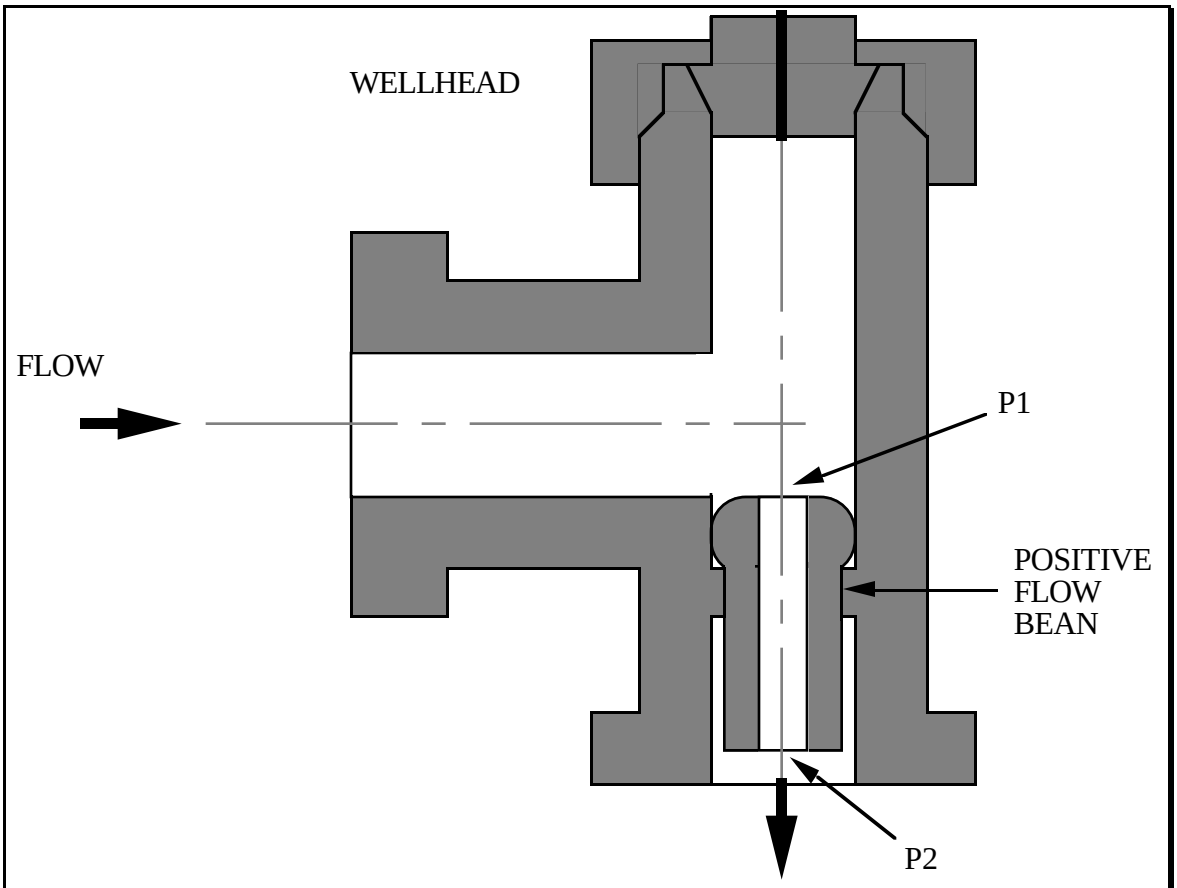

Figure 4.1: Positive Choke (from Golan and Whitson, 1986).

- maintain stable pressure downstream of the choke for processing equipment;
- provide the necessary backpressure on a reservoir to avoid formation damage and to prevent sand from entering the wellbore;
- prevent gas and/or water coning;
- control flow rates and maintain well allowables; and
- produce the reservoir at the most efficient rate.

By introducing a surface choke, operators can effectively isolate the reservoir component from the surface processing component.

Surface chokes are capable of two modes of flow: critical and subcritical. Critical flow occurs when the velocity through the choke is greater than the sonic velocity of the fluid resulting in a Mach number for the fluid that is greater than or equal to one. Recall that a pressure disturbance travels at the sonic velocity. Therefore, if the velocity of the fluid is greater than the sonic velocity of the fluid, any downstream perturbation is unable to propagate upstream and the mass flow rate through the choke is solely a function of the upstream parameters. As can be seen from Figure 4.2, there exists a certain critical pressure ratio below which the mass flow rate is constant, regardless of the downstream pressure.

Although correlations for single-phase flow across chokes are well developed, accurate correlations for multiphase flow across chokes are rare. Of the correlations that are available, most are strictly for critical flow. A few correlations make attempts at modeling subcritical flow but fall short of their objectives. The present state-of-the-art for modeling subcritical multiphase flow through chokes is disappointing at best.

The procedure of nodal analysis avoids the problem of modeling the binary flow behavior of surface chokes by assuming that chokes are always in critical flow. Nodal analysis will then use one of the many empirical choke equations to account for all well conditions. While this is an acceptable solution most of the time at relatively little computational expense, it simply does not provide an accurate model of surface choke behavior.

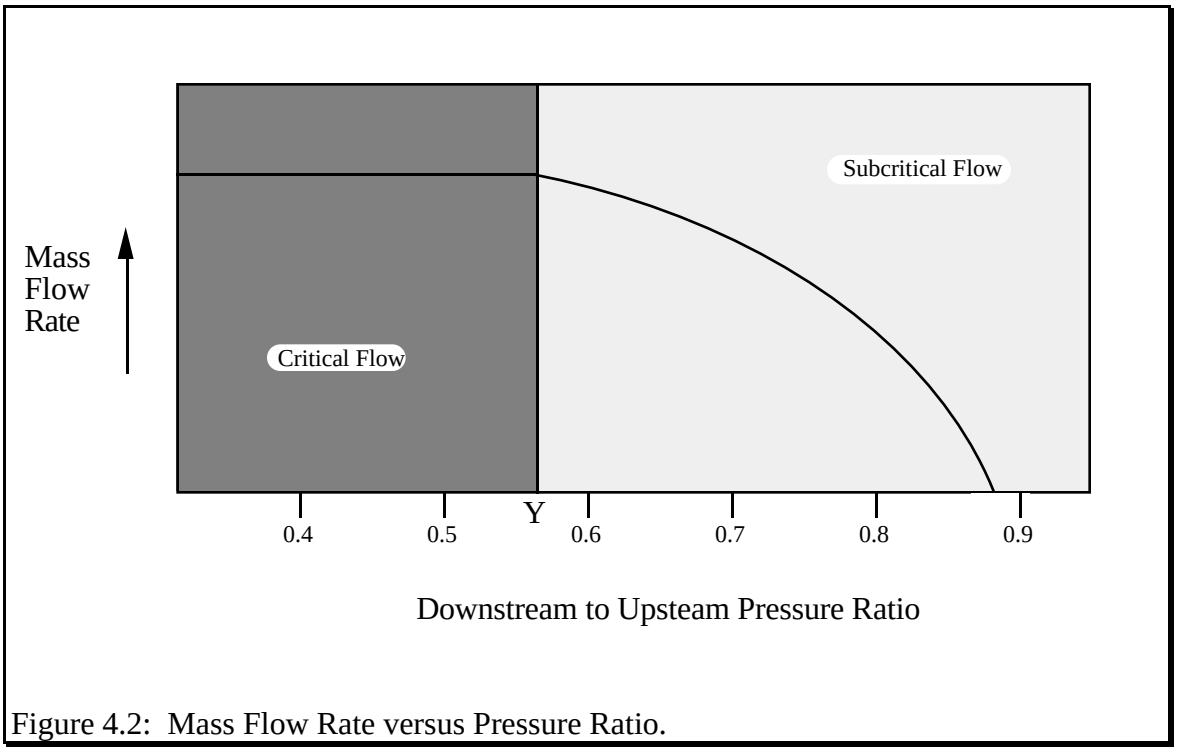

Figure 4.2: Mass Flow Rate versus Pressure Ratio.

4.1 Literature Review

Tangeren *et al*. (1949) were among the first to publish significant findings on multiphase flow through chokes. The importance of their research was that it demonstrated that for a compressible mixture, there exists a critical flow velocity above which pressure fluctuations cannot be transmitted upstream.

Gilbert (1954) published a simple formula based on daily production data of a California oil field that related the liquid flow rate, the gas-liquid ratio, the choke diameter, and the upstream pressure. His equation is

$$P_{WH} = \frac{435\, R_P^{0.5}\, Q_L}{S^{1.89}} \qquad (4.1)$$

where

P_{WH} = flowing wellhead pressure, psia

R_P = producing gas-liquid ratio, Mscf/stb

Q_L = gross liquid rate, stbd

S = bean diameter, 64ths of an inch

If the gas-liquid ratio is considered constant, then the flowing wellhead pressure and the gross liquids production are linearly proportional to each other as

$$P_{WH} = K\, Q_L \tag{4.2}$$

where

$$K = \frac{435\ R^{0.5}}{S^{1.89}} \tag{4.3}$$

By inspection, it is apparent that Equation 4.3 is strictly for critical flow, due to the exclusion of all downstream parameters. Gilbert (1954) claimed that his equation was valid only when the upstream pressure was more than 1.7 times the downstream pressure ($P_2 / P_1 < 0.588$). He also noted that the formula was extremely sensitive to the choke diameter: errors of 1/128ths of an inch in the choke diameter can cause an error of 5 to 20% in the flowing wellhead pressure estimate.

Gilbert's (1954) work was followed by several researchers making modifications to his formula. The researchers included Baxendall (1957), Ros (1959), and Achong (1961). All of the formulas kept the same basic form of

$$P_{WH} = \frac{A\ R_P^B\ Q}{S^C} \tag{4.4}$$

where only the constants were changed. The values for the coefficients for the various researchers are listed in Table 4.1. Baxendall's revision (1957) of the Gilbert equation was simply an update of the coefficients based on incremental data. Ros (1959) extended the theoretical work of Tangeren (1949) and in the process formulated his own version of the Gilbert (1954) equation to match the particular data he was working with. Achong (1961) modified the Gilbert (1954) equation to match the performance of 104 wells in the Lake Maracaibo Field of Venezuela.

Several researchers have taken the treatment of choke performance beyond a purely empirical basis. Those of consequence include Ros (1960), Poetmann & Beck (1963),

Table 4.1: Empirical Coefficients for Two-Phase Critical Flow Correlations.			
Correlation	A	B	C
Gilbert (1954)	10.00	0.546	1.89
Baxendall (1957)	9.56	0.546	1.93
Ros (1959)	17.40	0.500	2.00
Achong (1961)	3.82	0.650	1.88

Omaña *et al*. (1969), Fortunati (1972), Ashford & Pierce (1975), and Sachdeva *et al.* (1986). It should be pointed out that only Fortunati (1972), Ashford & Pierce (1975), and Sachdeva *et al.* (1986) have attempted to model both critical and subcritical flow.

Ros (1960) extended the work of Tangeren (1949) to account for mist flow where gas is the continuous phase. Ros (1960) demonstrated that accelerational effects dominate choke behavior and that slippage effects are negligible. Poetmann & Beck (1963) converted the Ros (1960) equation to field units and presented it as a series of nomographs.

Omaña *et al*. (1969) conducted experiments with water and natural gas flowing through restrictions. They performed a dimensional analysis that yielded eight dimensionless groups to characterize the flow. A regression analysis produced an empirical correlation based on five of these dimensionless groups. The Omaña (1969) correlation was never widely accepted because it was based on small diameters (4 to 14 / 64ths of an inch), low flow rates (800 bpd maximum), low pressure (400 to 1000 psig), and the correlation was developed for a water-gas mixture as opposed to an oil-gas mixture.

Fortunati (1972) demonstrated how to apply the findings of Guzhov and Medviediev (1962) to model the performance of a surface choke. Guzhov and Medviediev (1962) developed a curve relating the velocity of the mixture, V_M, to the pressure ratio of downstream pressure to upstream pressure, P_2 / P_1, where P_1 was constant at 19.8 psia. Fortunati (1972) showed how to correct the the mixture velocity for the actual downstream pressure. Having the corrected velocity of the mixture, the determination of the liquid

flowrate is straightforward. Fortunati's (1972) work was one of the first to be applicable to both critical and subcritical flow.

Ashford & Pierce (1975) presented an analytic method to determine critical and subcritical flow rates in subsurface safety valves. Their model was based on actual field tests and included oil and water flow, as well as free gas and solution gas. They derived an expression to predict the pressure ratio of downstream to upstream pressure, P_2 / P_1, at the critical-subcritical flow boundary. They assumed that the derivative of mass flow rate to the pressure ratio is zero at critical flow conditions. One of the shortcomings of the Ashford & Pierce (1975) model is their definition of the downstream pressure. Ideally, P_2 is the lowest pressure reached in the choke. In practice, this pressure cannot be easily measured and without uncertainty.

4.2 The Sachdeva *et al.* (1986) Choke Model

One of the most recent treatments of the choke problem was performed by Sachdeva *et al*. (1986). The premise of their work is the determination of the critical pressure ratio and is an extension of the work of Ashford & Pierce (1975). In their 1986 paper, Sachdeva *et al*. (1986) outline a procedure to determine the critical pressure ratio as well as the actual pressure ratio.

Although the Sachdeva *et al.* (1986) model is, perhaps, the best method we currently have at our disposal, it nevertheless is rife with limiting assumptions. Some of these assumptions are

- the gas phase contracts isentropically but expands polytropically;
- flow is one-dimensional;
- phase velocities are equal at the throat (no slippage occurs between the phases);
- the predominant influence on pressure is accelerational;
- the quality of the mixture is constant across the choke (no mass transfer between the phases);
- the liquid phase is incompressible.

Moreover, the Sachdeva *et al.* (1986) model makes no attempt to distinguish between free gas and solution gas, nor does it take into account the effect of different mixtures of liquids. Despite all of its apparent shortcomings, the Sachdeva *et al.* (1986) model is, relatively speaking, one the best available.

The first step of the Sachdeva *et al*. (1986) approach is to locate the critical-subcritical flow boundary. This is done by iterating and converging on Y_C in the expression

$$Y_C = \left[\frac{\frac{K}{K-1} + \frac{(1 - X_1) V_L (1 - Y_C)}{X_1 V_{G1}}}{\frac{K}{K-1} + \frac{N}{2} + \frac{N (1 - X_1) V_L}{X_1 V_{G2}} + \frac{N}{2}\left[\frac{(1 - X_1) V_L}{X_1 V_{G2}}\right]^2} \right]^{\left(\frac{K}{K-1}\right)} \tag{4.5}$$

Use the critical pressure ratio to determine the critical mass flux

$$G_C = C_D \left\{ 2\, g_C\, 144\, P_1\, \rho_{M2}^2 \left[\frac{(1 - X_1)(1 - Y_C)}{\rho_L} + \frac{X_1 K}{K-1} (V_{G1} - Y_C V_{G2}) \right] \right\}^{0.5} \tag{4.6}$$

and use the upstream parameters to determine the mass flux at upstream conditions as

$$G_1 = \frac{\rho_G Q_G + 5.615 \rho_L Q_L}{150 \pi D_{CH}^2} \tag{4.7}$$

Compare the upstream mass flux with the critical mass flux. If the mass flux is greater than the critical mass flux, $G_1 \geq G_C$, then we are in the critical flow region and the *maximum* downstream pressure is

$$P_2 = Y_C P_1 \tag{4.8}$$

If the calculated mass flux is less than the critical mass flux, $G_1 < G_C$, then we are in the subcritical flow region. The downstream pressure may be found by solving for the root of the expression $(G_1 - G_2)$, where G_2 is found with the equations

$$Y = \frac{P_2}{P_1} \tag{4.9}$$

$$V_{G2} = V_{G1} Y^{\left(-\frac{1}{K}\right)} \tag{4.10}$$

$$\rho_{M2} = (X_1 V_{G2} + (1 - X_1) V_L)^{-1} \tag{4.11}$$

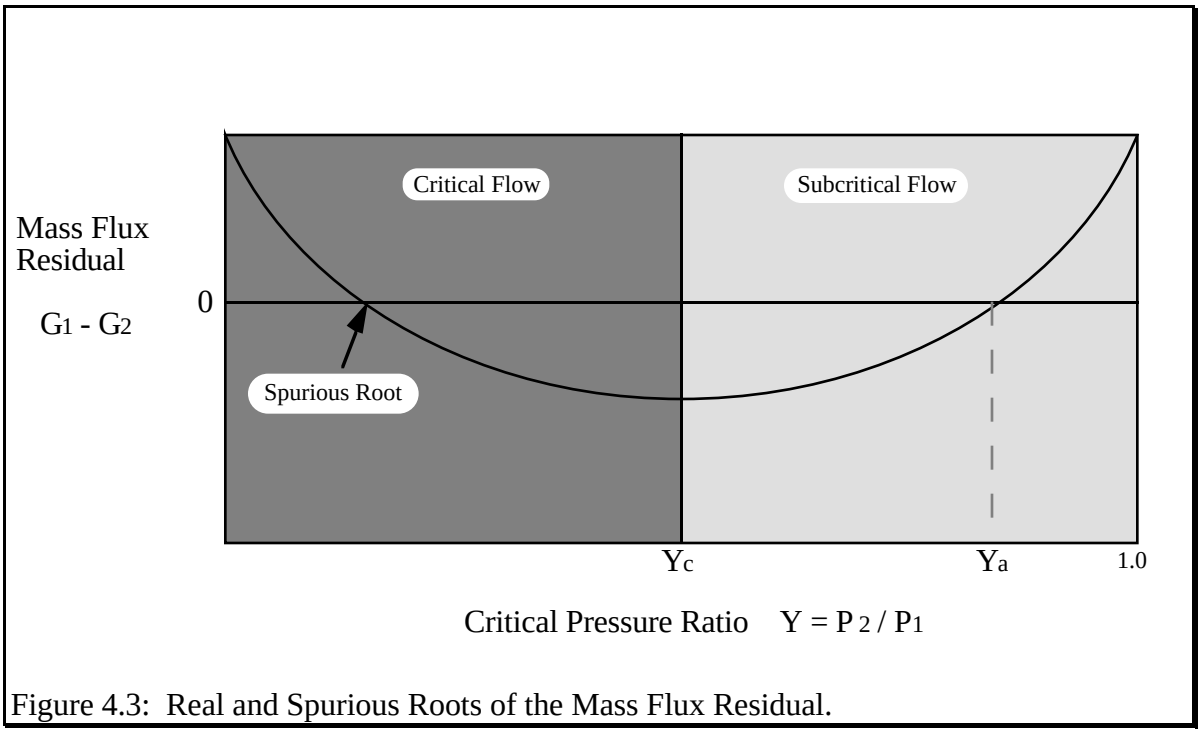

Figure 4.3: Real and Spurious Roots of the Mass Flux Residual.

$$G_2 = C_D \left\{ 2\, g_C\, 144\, P_1\, \rho_{M2}^2 \left[\frac{(1 - X_1)(1 - Y)}{\rho_L} + \frac{X_1\, K}{K - 1} (V_{G1} - Y\, V_{G2}) \right] \right\}^{0.5} \qquad (4.12)$$

The expression G_1-G_2 is a parabolic function as illustrated in Figure 4.3. We know that the root we are searching for lies somewhere between Y_C and one. Since the expression $\{G_1 - G_2\}$ has two roots, one above Y_C and one below Y_C, care must be taken to converge to the proper root. Several routines exist which allow the user to constrain the range for the solution. This study used Brent's Method (Press *et al.*, pg. 251) with the solution constrained between Y_C and one. When the proper root of the expression has been found, the actual pressure ratio will be known and the downstream pressure may be solved for with Equation 4.8.

Chapter 5

PHASE SEPARATION

The well stream that arrives at the surface consists of multiple phases such as oil, gas, water, and possibly sand. Before the hydrocarbon well stream may be directed to storage facilities or delivered to market, it must first be separated into the discrete phases present. Gas pipelines stipulate maximum levels of water vapor content and contaminants. Oil purchase contracts specify the maximum amount of basic sediment and water that is allowable in the crude.

The most common form of isolating the gas and liquid phases present in a well stream is to pass the stream through a separator (see Figure 5.1). A separator is typically maintained at a constant operating pressure by controlling the effluence from the separator with backpressure valves. A separator is designed to provide sufficient time for the various phases of the well stream to equilibrate and separate by means of gravity

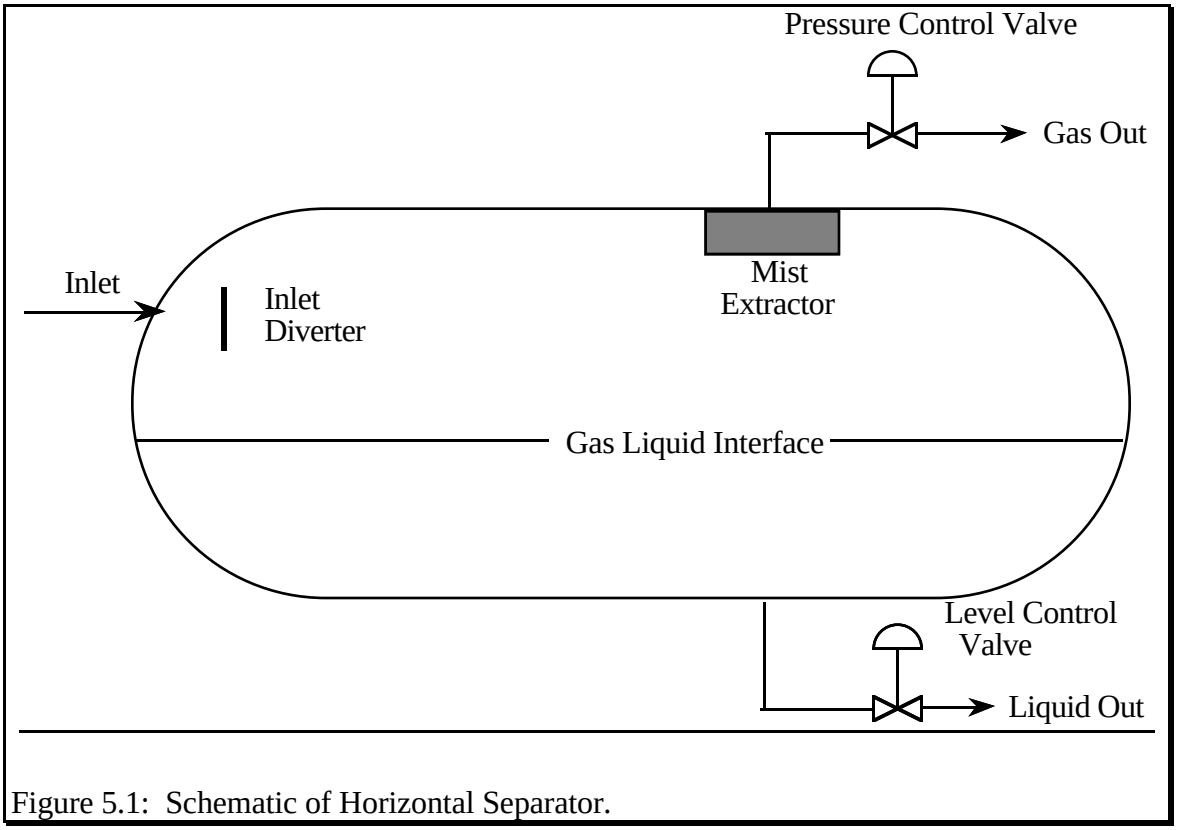

Figure 5.1: Schematic of Horizontal Separator.

segregation. The gas phase must exit from the top of the separator whereas the liquid phase must exit from the bottom. The resulting gas may then be passed to a glycol dehydrator for further removal of water vapor and contaminants before being delivered to a pipeline. The liquid stream coming out of a separator may be passed through additional separators operating at successively lower pressures before finally being delivered to the stock tank (see Figure 5.2). Alternatively, the liquid stream may be passed through gunbarrels, free water knock-outs, skim tanks, and heater treaters depending on the specific treating requirements. Any solids present in the well stream are usually removed by the force of gravity which may be augmented by hydrocyclones.

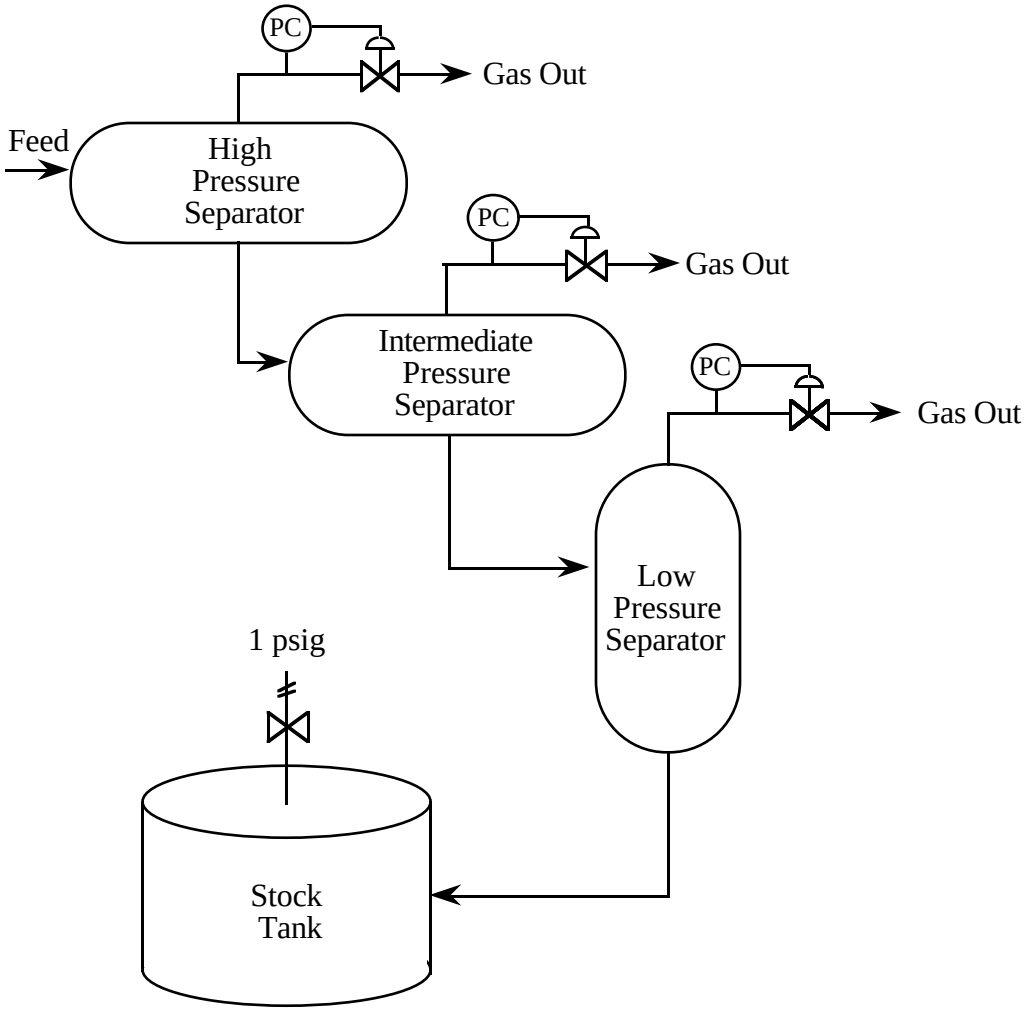

Figure 5.2: Stage Separation (from Arnold 1986).

5.1 Optimization of Phase Separation

The optimization of phase separation practices is important because by varying the blend of surface oil and gas produced per reservoir volume, an operator may markedly affect the total value of the mix. The total value of the mix is affected by the fractional volumes produced of each phase as well as the quality of each phase. The fractional volume of each phase is important because traditionally the market has paid a significant premium for hydrocarbons in the liquid phase. At times, the vapor phase was considered to be of no economic value, prompting operators to flare the gas rather than attempt to find a market for it. In addition to the gross volume produced of the oil and gas phases, the total value is affected by the quality of the phases. A gas price is adjusted for the BTU content while the price paid for crude varies with the API gravity of the oil.

An important concept in surface phase separation is that the fractional liquid recovery will always be enhanced by adding more separators between the wellhead and the stock tank. By increasing the number of separators, the liberation process between the wellhead and the stock tank is essentially transformed from a flash liberation process to a differential liberation process, thus improving the fractional liquid recovery. In a stage separation process, the light hydrocarbons molecules that flash are removed at relatively high pressure, keeping the partial pressure of the intermediate hydrocarbons lower at each stage. As the number of stages approaches infinity, the lighter molecules are removed as soon as they are formed and the partial pressure of the intermediate components is maximized at each stage.

An equally important concept is that for a finite number of separators, there is an optimal combination of discrete separator pressures that will maximize the fractional liquids recovery. At the optimal combination of separator pressures, the API gravity of the crude will be maximized and the gas-oil ratio will minimized (see Figure 5.3).

To mimic the behavior of surface facilities, this study elected to model the performance of a two-stage separation process. A two-stage separation process involves flashing the well stream initially at the separator operating conditions and then flashing the resulting liquid stream at stock tank conditions. Assuming the temperatures of the two stages to be constant and by setting the stock tank pressure to atmospheric pressure, the separator pressure can be optimized to yield the most beneficial mix of oil and gas fractional recoveries.

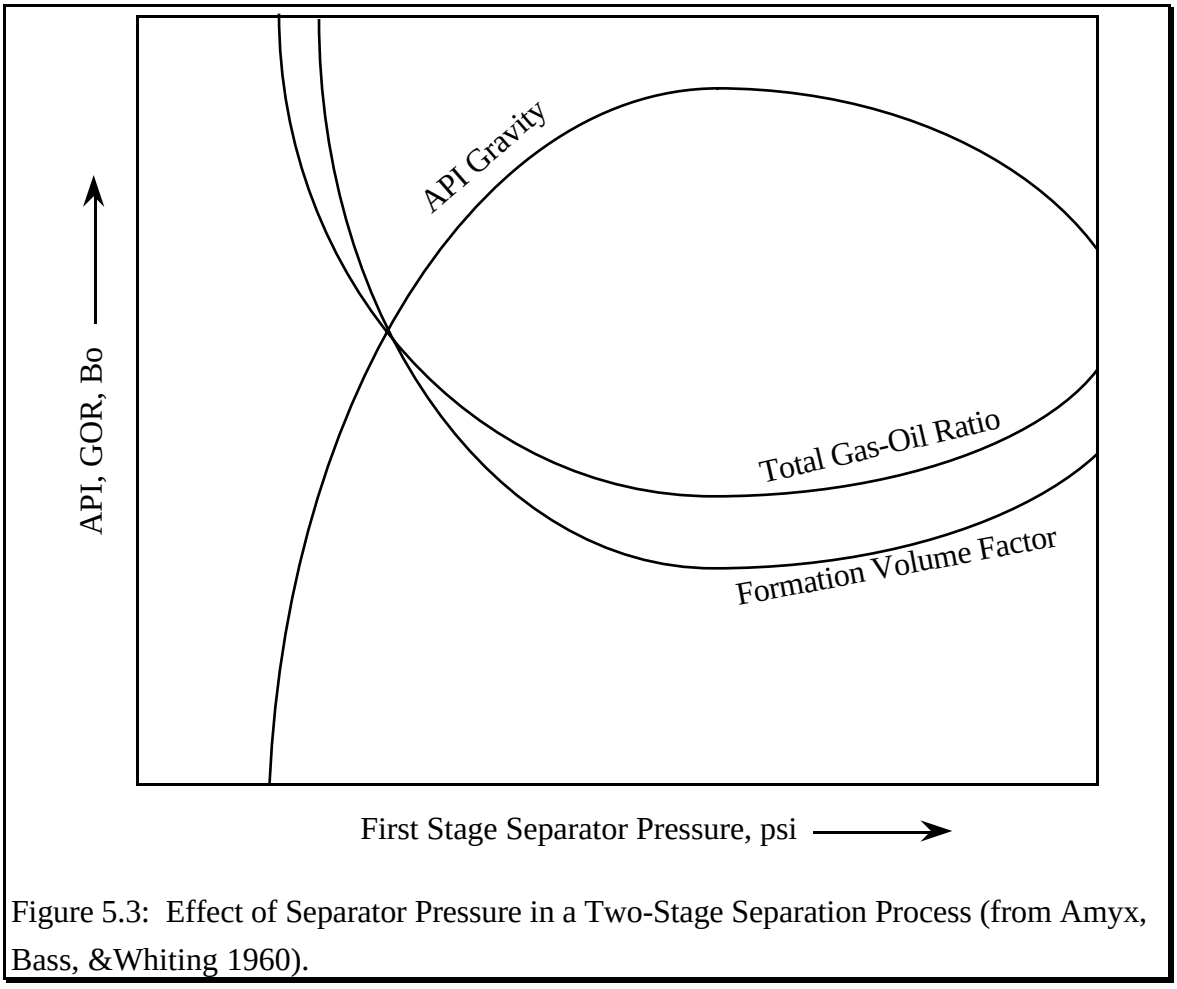

Figure 5.3: Effect of Separator Pressure in a Two-Stage Separation Process (from Amyx, Bass, &Whiting 1960).

5.2 Flash Equilibria

A mixture is flashed by being suddenly exposed to a new temperature and pressure at which it must re-equilibrate. A flash calculation takes the overall composition of a mixture and determines the resulting phase equilibria at a new temperature and pressure, such as the number of phases present and the composition and amount of each phase. The procedure of performing a flash calculation is iterative and converges when the fugacity of each component is the same in both phases. The basic procedure of a flash calculation involves six steps:

1) Given the composition of the mixture, Z_i, at a temperature T and pressure P, guess the resulting compositions of the gas and liquid phases, Y_i and X_i respectively.

2) Calculate the equation of state parameters.

3) Solve the equation of state for the fractional molar volumes of vapor and liquid, V^V and V^L respectively.

4) Determine the partial fugacities of the components in each phase, $\hat{f}_i^V$ and $\hat{f}_i^L$ respectively.

5) Check if the ratio of the fugacities for each component has converged to a value of one, i.e. abs $\left(\hat{f}_i^V / \hat{f}_i^L\right) \leq (1+\varepsilon)$. If the ratio for each component has converged to a value of one then equilibrium between the two phases has been achieved.

6) If the fugacity ratio has not converged to one for each component, then improve the estimates for the phase compositions, Yi and Xi, and proceed with step 2.

5.2.1 Initial Estimate of Phase Compositions

The ratio of the vapor mole fraction to the liquid mole fraction for a given component is known as the equilibrium ratio, or alternatively as the K-value, and is defined as

$$K_i \equiv Y_i / X_i \tag{5.1}$$

Empirical correlations can be used to provide an initial estimate of the equilibrium ratios. The Wilson equation (1962) was used in this model

$$K_i = \frac{\exp\left[\, 5.37\,(\,1 + \omega_i\,)\left(\,1 - \frac{1}{T_{ri}}\right)\right]}{P_{ri}} \tag{5.2}$$

where

$$T_{ri} = T / T_{ci}$$

$$P_{ri} = P / P_{ci}$$

and ω_i is the acentric factor for component i and is available in the literature. Performing a material balance on component i we know that

$$Z_i = X_i L + Y_i V \tag{5.3}$$

where V and L are the vapor and liquid mole fractions and L = 1 - V. Using the relation Yi = Ki / Xi and solving for Xi yields

$$X_i = \frac{Z_i}{L + (1 - L) K_i} \tag{5.4}$$

and letting Xi = Yi / Ki and solving for Yi yields

$$Y_i = \frac{K_i Z_i}{L + (1 - L) K_i} \tag{5.5}$$

Noting the constraint of

$$\sum_i X_i - \sum_i Y_i = 0 \tag{5.6}$$

we must find a solution to the equation

$$F(L) = \sum_i \frac{Z_i (1 - K_i)}{K_i + (1 - K_i) L} = 0 \tag{5.7}$$

This equation can be efficiently solved with Newton-Raphson iteration where

$$L^{k+1} = L^k - \frac{F(L^k)}{\left.\frac{\partial F}{\partial L}\right|_{L^k}} \tag{5.8}$$

and convergence is achieved when both

1) $\text{abs}\left(L^{k+1} - L^k\right) < \varepsilon$

2) $F\left(L^{k+1}\right) < \varepsilon$

where ε is a small tolerance. In this study, ε was set equal to 10^{-10}. Once L is determined, the compositions of the liquid and vapor phases are obtained from Equations 5.4 and 5.5.

The number of phases present is determined by considering Equation 5.7. At the dew point, where L = 0, Equation 5.7 yields

$$\sum_i \frac{Z_i}{K_i} = 1 \tag{5.9}$$

Likewise, at the bubble point, where L = 1, Equation 5.7 yields

$$\sum_i K_i Z_i = 1 \tag{5.10}$$

Two phases are present when

$$\sum_i K_i Z_i > 1 \tag{5.11}$$

$$\sum_i \frac{Z_i}{K_i} > 1 \tag{5.12}$$

5.2.2 Calculate Equation of State Parameters

One of the most popular equation of states in use today is the Redlich-Kwong equation of state as modified by Soave (1972). The standard form of the Soave-Redlich-Kwong (SRK) equation of state is

$$P = \frac{RT}{V-b} - \frac{a\alpha}{V(V-b)} \tag{5.13}$$

where

$$a = \frac{0.42748 R^2 T_c^2}{P_c} \tag{5.14}$$

$$b = \frac{0.8664\ R\ T_c}{P_c} \tag{5.15}$$

$$\alpha = \left[1 + \left(0.48508 + 1.55171\omega - 0.15613\ \omega^2\right)\left(1 - T_r^{0.5}\right)\right]^2 \tag{5.16}$$

The SRK equation of state may be expressed in cubic form as

$$V^3 - \frac{RT}{P}V^2 + \frac{1}{P}\left((a\alpha)_m - b_m R T - P b_m^2\right)V - \frac{(a\alpha)_m b_m}{P} = 0 \tag{5.17}$$

where

$$(a\alpha)_m = \sum_i \sum_j Y_i Y_j (a\alpha)_{ij} \quad (5.18)$$

$$b_m = \sum_i Y_i b_i \quad (5.19)$$

$$(a\alpha)_{ij} = (1 - K_{ij}) \sqrt{(a\alpha)_i (a\alpha)_j} \quad (5.20)$$

where Kij are the binary interaction parameters and may be obtained from Table 5.1.

Table 5.1: Binary Interaction Parameters for the Soave Equation (Prausnitz 1986).

	H_2S	CO_2	N_2	CO
H_2S	---	0.102	0.140	---
CO_2	0.102	---	-0.022	-0.064
N_2	0.140	-0.022	---	0.046
CO	---	-0.064	0.046	---
Methane	0.0850	0.0973	0.0319	0.03
Ethane	0.0829	0.1346	0.0388	0.00
n-Propane	0.0831	0.1018	0.0807	0.02
2-Methylpropane	0.0523	0.1358	0.1357	---
n-Butane	0.0609	0.1474	0.1007	---
2-Methylbutane	---	0.1262	---	---
n-Pentane	.0.697	0.1278	---	---
n-Hexane	---	---	0.1444	---
n-Heptane	0.0737	0.1136	---	---
n-Octane	---	---	---	0.10
n-Nonane	0.0542	---	---	---
n-Decane	0.0464	0.1377	0.1293	---
Propylene	---	0.0914	---	---
Cyclohexane	---	0.1087	---	---
Isopropylcyclohexane	0.0562	---	---	0.01
Benzene	---	0.0810	0.2131	---
1,3,5-Trimethylbenzene	0.0282	---	---	---

5.2.3 Solve Equation of State for V^L and V^V

The cubic form of the SRK equation of state must be solved for the liquid and vapor molar volumes. An analytical solution was used to solve the cubic equation as follows. For a cubic equation of the form

$$V^3 + A_2 V^2 + A_1 V + A_0 = 0 \tag{5.21}$$

let

$$\psi = V + A_2 / 3 \tag{5.22}$$

$$\Omega = \frac{1}{3}\left(3 A_1 - A_2 \right) \tag{5.23}$$

$$\delta = \frac{1}{27}\left(2 A_2^3 - 9 A_2 A_1 + 27 A_o \right) \tag{5.24}$$

$$\mu = \left(-\frac{\delta}{2} - \sqrt{\frac{\delta^2}{4} + \frac{\Omega^3}{27}} \right)^{1/3} \tag{5.25}$$

$$\lambda = \left(-\frac{\delta}{2} + \sqrt{\frac{\delta^2}{4} + \frac{\Omega^3}{27}} \right)^{1/3} \tag{5.26}$$

The roots of the cubic equation are

one real and two imaginary roots if $\frac{\delta^2}{4} + \frac{\Omega^3}{27} > 0$,

three real (two equal) roots if $\frac{\delta^2}{4} + \frac{\Omega^3}{27} = 0$,

or three real and nonequal roots if $\frac{\delta^2}{4} + \frac{\Omega^3}{27} < 0$.

For three real roots, let

$$\cos\theta = \frac{-\delta}{\sqrt{-\frac{4\Omega}{27}}} \tag{5.27}$$

Then

$$\psi_1 = 2 \cos\frac{\theta}{3}\sqrt{-\frac{\Omega}{3}} \tag{5.28}$$

$$\psi_2 = 2\left(\cos\frac{\theta}{3} + \frac{2\pi}{3}\right)\sqrt{-\frac{\Omega}{3}} \tag{5.29}$$

$$\psi_3 = 2\left(\cos\frac{\theta}{3} + \frac{4\pi}{3}\right)\sqrt{-\frac{\Omega}{3}} \tag{5.30}$$

5.2.4 Determine Partial Fugacities

For the Soave-Redlich-Kwong equation of state, the partial fugacity of component i is given by

$$\hat{f}_i = P \exp\left[\left(\frac{V}{V-b_m}\right) + \frac{b_i}{V - b_m} + \frac{2\sum(Y_i\, a_{ij})}{R\,T\,b_m}\ln\left(\frac{V+b_m}{V}\right) + \frac{(a\alpha)_m\, b_i}{R\,T\,b_m^2}\left(\ln\left(\frac{V+b}{V}\right) - \frac{b_m}{V+b_m}\right) - \ln\left(\frac{P\,V}{Y_i\,R\,T}\right)\right] \tag{5.31}$$

5.2.5 Convergence Check

A solution is found when the partial fugacity of each component is the same across all phases.

$$\frac{\hat{f}_i^V}{\hat{f}_i^L} = 1 \qquad \text{for all i} \tag{5.32}$$

Since the algorithm is iterative, an exact solution is difficult if not impossible to achieve. Instead, we must test if we are within some tolerance of this requirement. The convergence criterion used in this study was whether the fugacity ratio for each component was within a tolerance of ε of one:

$$\text{abs}\left(\hat{f}_i^V / \hat{f}_i^L\right) \le 1 + \varepsilon \tag{5.33}$$

If the convergence criterion is met then the phase compositions and molar volumes are known.

5.2.6 Modify the Vapor and Liquid Compositions

For the purposes of this study, a successive substitution scheme was used to estimate new equilibrium ratios for successive iterations. The fugacity coefficient is defined as

$$\hat{\phi}_i^V = \frac{\hat{f}_i^V}{Y_i P} \tag{5.34}$$

$$\hat{\phi}_i^L = \frac{\hat{f}_i^L}{Y_i P} \tag{5.35}$$

It follows that

$$\frac{\hat{\phi}_i^L}{\hat{\phi}_i^V} = \frac{\hat{f}_i^L}{\hat{f}_i^V} \frac{Y_i}{X_i} \tag{5.36}$$

At equilibrium, the partial fugacities are equal. The equation simplifies to

$$\frac{\hat{\phi}_i^L}{\hat{\phi}_i^V} = \frac{Y_i}{X_i} \tag{5.37}$$

which is simply the definition of the equilibrium ratio. Therefore, we can used the fugacity coefficients determined in the current unsuccessful iteration to estimate new K-values.

$$k_i^{k+1} = \frac{\hat{f}_i^L}{\hat{f}_i^V} k_i^k \tag{5.38}$$

The new K-values are used to restart the procedure.

Chapter 6

NONLINEAR OPTIMIZATION

There are numerous problems for which people strive to find an optimal solution. These problems might be minimizing the fuel consumption of an engine, maximizing the efficiency of a process, or minimizing the volume occupied by a cluster of objects. It is trivial to optimize a problem that depends on a single variable. It is when several variables are optimized simultaneously that matters become complicated.

Mathematics can provide a powerful tool to optimize a problem, regardless of the number of variables involved. Numerical optimization is the location of the extrema of a mathematical model. The mathematical model, referred to as the objective function, accepts multiple decision variables as input and returns a single value, the objective variable, as output. Optimization strives to locate the minimum or maximum value of the objective function.

Nonlinear optimization methods based on Newton's technique locate the extrema by approximating the objective function with a nonlinear quadratic model. Let the objective function, F, be a nonlinear function of the vector of decision variables, $\tilde{x}$.

$$F = f(\tilde{x}) \tag{6.1}$$

Newton's method approximates the nonlinear objective function, F, with a quadratic model, Q, which is also a function of the vector of decision variables, $\tilde{x}$.

$$Q(\tilde{x}) \approx F(\tilde{x}) \tag{6.2}$$

The quadratic approximation

$$Q(\tilde{x}) = c^T\tilde{x} + \frac{1}{2}\tilde{x}^T \mathbf{G}\, \tilde{x} \tag{6.3}$$

may be conceptualized, in two dimensions, as a bowl. If the matrix **G** is negative-definite, the expression is bounded above and unbounded below (the bowl is upside-down) and will therefore have a maximum (See Figure 6.1). Conversely, if the matrix **G** is positive definite, the expression is bounded below and unbounded above (the bowl is right-side-up)

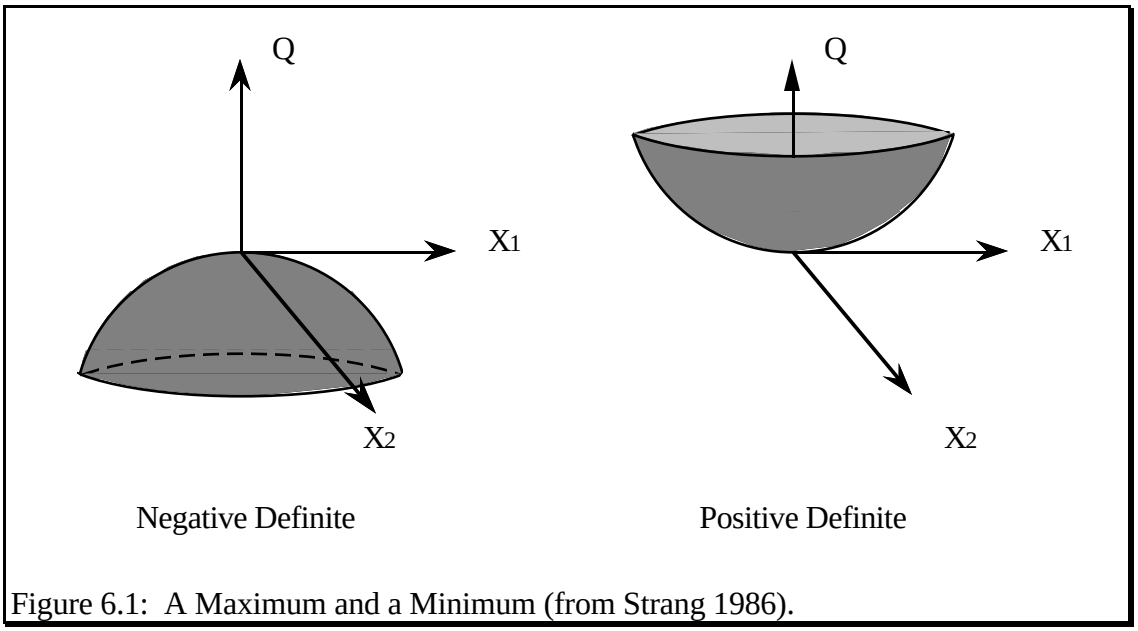

Figure 6.1: A Maximum and a Minimum (from Strang 1986).

and will have a minimum. If **G** is indefinite, the expression is unbounded both above and below and therefore does not have an extrema.

To find a minimum of an objective function, a positive definite matrix should be used. Likewise, to find a maximum of an objective function, a negative definite matrix should be used. However, in all of the literature pertaining to optimization, the convention is to always frame the problem in terms of finding the minimum of a function. Therefore, instead of maximizing a function, the convention is to minimize the negative of the objective function. Thus, even for maximizing a function, we will speak of 'descending' to the minimum.

For a problem that is inherently nonlinear, nonlinear approximations of the objective function allow the solution to be found at a much faster rate than with linear approximations. In contrast, the much heralded linear programming approximates the objective function with linear models. Since a linear relationship is unbounded in all directions (unless it is constant), a minimum or maximum value cannot occur without some form of constraint. Thus, the solution to a linear programming problem can only occur at the intersection of a linear approximation and a constraint. This is the principle that the Simplex algorithm is based upon.

The theory of optimization is very well developed. Optimization routines are widely available through software libraries such as the Numerical Algorithms Group and

IMSL (1987). For a broad overview of numerical optimization techniques, see Gill, Murray, & Wright (1981). For a more extensive treatment of numerical optimization applied to petroleum engineering problems, see Barua (1989).

6.1 Newton's Method

Newton's Method is one of the most common techniques used in nonlinear optimization. It is the standard against which all other algorithms are measured. If Newton's Method is provided with a good initial estimate of the solution, quadratic convergence is achieved.

Newton's Method achieves this rate of convergence by approximating the objective function with a quadratic model. The quadratic model is chosen so that, at a given point, its first and second derivatives are identical to the first and second derivatives of the objective function. Therefore, at the given point, the objective function and the quadratic model are identical in value, slope, and curvature. The quadratic model is solved for the stationary point where its gradient goes to zero. If the quadratic model is a good approximation of the objective function, then the stationary point of the quadratic model should be near a stationary point of the objective function. The stationary point of the quadratic model is taken as the new estimate of the objective function's stationary point and the process is repeated until some form of convergence criteria is satisfied.

Taylor's theorem provides the mathematical basis for Newton's Method. Taylor's theorem states that if a function and its derivatives are known at a single point, then approximations to the function can be made at all points in the immediate neighborhood of the point. The Taylor series expansion of a general function F about $\tilde{x}$ gives a simple approximation to the function F in the immediate neighborhood of $\tilde{x}$ as

$$F(\tilde{x}+\tilde{p}) = F(\tilde{x}) + \tilde{g}^T \tilde{p} + \frac{1}{2} \tilde{p}^T \mathbf{H} \tilde{p} + O\left(\|\tilde{p}\|^3\right) \tag{6.4}$$

where $\tilde{x}$ is the vector of variables,

$$\tilde{x} = \begin{bmatrix} x_1 \\ x_2 \\ x_3 \\ \cdots \\ x_n \end{bmatrix} \tag{6.5}$$

$\tilde{p}$ is the vector of displacement from $\tilde{x}$,

$$\tilde{p} = \begin{bmatrix} \Delta x_1 \\ \Delta x_2 \\ \Delta x_3 \\ \cdots \\ \Delta x_n \end{bmatrix} \tag{6.6}$$

$\tilde{g}$ is the gradient *n*-vector of $\tilde{x}$,

$$\tilde{g} = \begin{bmatrix} \frac{\partial F}{\partial x_1} \\ \frac{\partial F}{\partial x_2} \\ \frac{\partial F}{\partial x_3} \\ \cdots \\ \frac{\partial F}{\partial x_n} \end{bmatrix} \tag{6.7}$$

and **H** is the Hessian matrix of $\tilde{x}$,

$$\mathbf{H} = \begin{bmatrix} \frac{\partial^2 F}{\partial x_1 \partial x_1} & \frac{\partial^2 F}{\partial x_1 \partial x_2} & \frac{\partial^2 F}{\partial x_1 \partial x_3} & \cdots & \frac{\partial^2 F}{\partial x_1 \partial x_n} \\ \frac{\partial^2 F}{\partial x_2 \partial x_1} & \frac{\partial^2 F}{\partial x_2 \partial x_2} & \frac{\partial^2 F}{\partial x_2 \partial x_3} & \cdots & \frac{\partial^2 F}{\partial x_2 \partial x_n} \\ \frac{\partial^2 F}{\partial x_3 \partial x_1} & \frac{\partial^2 F}{\partial x_3 \partial x_2} & \frac{\partial^2 F}{\partial x_3 \partial x_3} & \cdots & \frac{\partial^2 F}{\partial x_3 \partial x_n} \\ \cdots & \cdots & \cdots & \cdots & \cdots \\ \frac{\partial^2 F}{\partial x_n \partial x_1} & \frac{\partial^2 F}{\partial x_n \partial x_2} & \frac{\partial^2 F}{\partial x_n \partial x_3} & \cdots & \frac{\partial^2 F}{\partial x_n \partial x_n} \end{bmatrix} \tag{6.8}$$

Considering only the first and second order terms of the Taylor's series expansion (Equation 6.4) gives a quadratic approximation of the function F in the neighborhood of $\tilde{x}$ as

$$Q(\tilde{x}+\tilde{p}) = F(\tilde{x}) + \tilde{g}^T \tilde{p} + \frac{1}{2} \tilde{p}^T \mathbf{H} \tilde{p} \tag{6.9}$$

The minimum of a function can occur only where the gradient vector vanishes and the gradient vector vanishes only at a stationary point. To find the stationary point of the quadratic approximation, we take the gradient of Q

$$\frac{\partial Q}{\partial \tilde{x}} = \tilde{g} + \mathbf{H}\,\tilde{p} \tag{6.10}$$

and equate this to zero. The resulting equation

$$\mathbf{H}\,\tilde{p} = -\,\tilde{g} \tag{6.11}$$

can only be satisfied by a stationary point. To solve for the step-direction $\tilde{p}$ that will lead to the stationary point, the Hessian must be inverted

$$\tilde{p} = -\,\mathbf{H}^{-1}\,\tilde{g} \tag{6.12}$$

The step-direction $\tilde{p}$ indicates the displacement from the point $\tilde{x}$ that would give the stationary point of the quadratic model. The Newton step is defined as the product $(\rho\,\tilde{p})$ where ρ is the scalar step-length and $\tilde{p}$ is the step-direction vector. We can update our estimate of the point $\tilde{x}$ by taking a Newton step

$$\tilde{x} \leftarrow \tilde{x} + \rho\,\tilde{p} \tag{6.13}$$

Thus, the method takes a step of length ρ in the $\tilde{p}$ direction. In unmodified Newton's Method, the length of the Newton step is implicitly taken as unity.

If the objective function is quadratic in form, then the quadratic approximation is exact and Newton's Method will converge to the stationary point in a single iteration. In the more likely event that the objective function is not quadratic in form, the higher-order terms that were ignored in the Taylor series expansion will become negligible as Newton's Method begins to converge on the stationary point. As the higher-order terms go to zero, the quadratic model will provide a very good approximation to the local surface and the method will approach quadratic convergence.

A key insight to Newton's Method can be obtained by investigating the eigensystem of the Hessian matrix. By performing spectral decomposition of the Hessian

$$\mathbf{H} = \mathbf{V}\,\Lambda\,\mathbf{V}^{T} \tag{6.14}$$

we obtain **V**, the matrix of eigenvectors, and Λ, the diagonal matrix of eigenvalues. Since the Hessian is symmetric and **V** is unitary, the inverted Hessian is given as

$$\mathbf{H}^{-1} = \mathbf{V}\,\Lambda^{-1}\,\mathbf{V}^{T} \tag{6.15}$$

Expressing the gradient as a linear combination of the eigenvectors,

$$\tilde{g} = \mathbf{V}\,\tilde{\alpha} \tag{6.16}$$

the step-direction is given by

$$\tilde{p} = -\,\mathbf{H}^{-1}\,\tilde{g} \tag{6.12}$$

$$= -\,\mathbf{V}\,\Lambda^{-1}\,\mathbf{V}^{T}\,\mathbf{V}\,\tilde{\alpha} \tag{6.17}$$

$$= -\,\mathbf{V}\,\Lambda^{-1}\,\tilde{\alpha} \tag{6.18}$$

$$= -\begin{bmatrix} \frac{v_1}{\lambda_1} & \frac{v_2}{\lambda_2} & \frac{v_3}{\lambda_3} & \cdots & \frac{v_n}{\lambda_n} \end{bmatrix}\tilde{\alpha} \tag{6.19}$$

Recall from linear algebra that an eigenvalue that is close to zero indicates that the function is close to being singular and therefore will change very little along the corresponding eigenvector. Equation 6.19 indicates that the smaller an eigenvalue is, the larger the step-direction will be in the direction of the corresponding eigenvector. Therefore, Newton's Method will take the largest strides in the directions that the function is least sensitive. While this feature is desirable with regard to convergence, it is extremely threatening to the stability of the algorithm if left unchecked. Since Newton's Method is only a quadratic approximation to the *local* surface of the objective function, all steps should be somewhat tentative.

The primary expense of Newton's Method is not the matrix solution (Equation 6.12), but the evaluation of the derivatives required for the gradient and the Hessian. If analytic expressions are unavailable for the derivatives, they must be evaluated using finite difference approximations. For *n* decision variables, $\left(\frac{n^2+n}{2}\right)$ second partial derivatives are necessary for the Hessian (recall that the Hessian is symmetric) and *n* first partial derivatives are necessary for the gradient. If e_i is the ith unit vector and h_i is the finite difference interval for the ith decision variable (see Figure 6.2), then the elements of the gradient are given by the expression

$$g_i = \frac{F(x+h_i e_i) - F(x-h_i e_i)}{2h_i} \tag{6.20}$$

The diagonal elements of the Hessian are given by

$$H_{ii} = \frac{F(x+h_i e_i) - 2F(x) + F(x-h_i e_i)}{h_i^2} \tag{6.21}$$

and the off-diagonal elements of the Hessian are given by

$$H_{ij} = \frac{F(x+h_i e_i+h_j e_j) + F(x-h_i e_i-h_j e_j) - F(x-h_i e_i+h_j e_j) - F(x+h_i e_i-h_j e_j)}{4h_i h_j} \tag{6.22}$$

All of the finite difference approximations are second-order accurate which preserves the second-order accuracy of the quadratic model. If first-order accuracy is acceptable in the mixed partial derivatives, significant savings can be realized by evaluating the off-diagonal elements of the Hessian as

$$H_{ij} = \frac{F(x+h_i e_i+h_j e_j) + F(x) - F(x+h_j e_j) - F(x+h_i e_i)}{h_i h_j} \tag{6.23}$$

Notice that after determining the elements of the gradient with Equation 6.20 and the diagonal elements of the Hessian with Equation 6.21, each off-diagonal element can be obtained with Equation 6.23 by a single additional function evaluation as opposed to the four additional function evaluations that would be required by Equation 6.22.

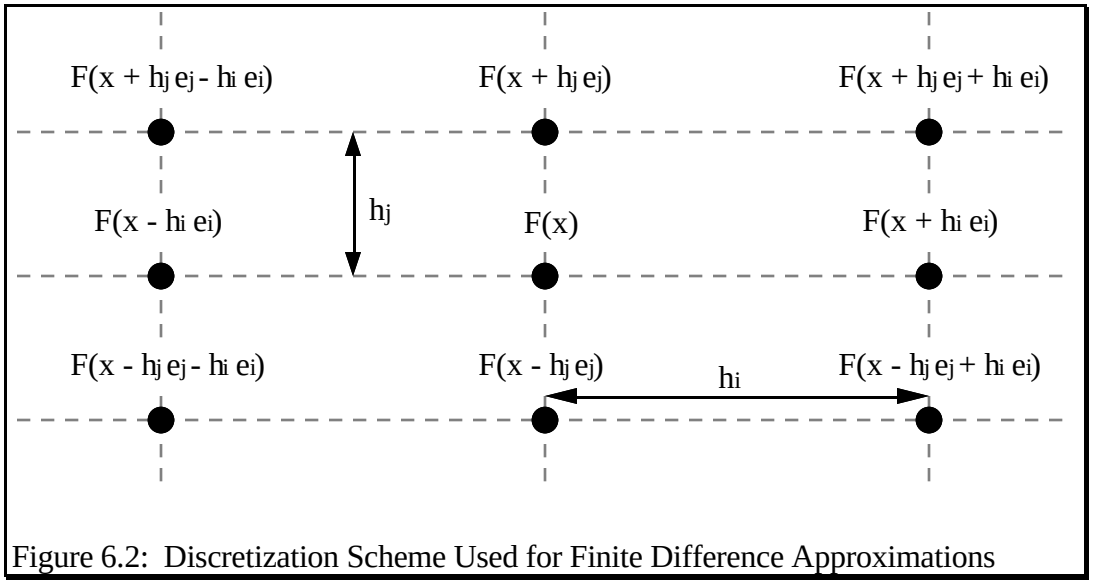

Figure 6.2: Discretization Scheme Used for Finite Difference Approximations

If used properly, Newton's Method offers the fastest rate of convergence available. However, this robust rate of convergence is achieved at the expense of the stability of the algorithm. Some of the shortcomings of the method are

- A good initial starting point is required for convergence. A poor estimate will result in divergence.
- If Newton's Method does converge, it converges to the nearest stationary point. No guarantee can be made that this is the desired stationary point. It could be a local minimum, a maximum, or a saddlepoint.
- The Hessian matrix is subject to numerical instabilities during the matrix solution.
- If the analytic derivatives are not available, the derivatives necessary to construct the gradient and Hessian will have to be evaluated by very costly finite difference approximations.

6.2 Modifications to Newton's Method

In practice, the first modification made to Newton's Method is to incorporate a one-dimensional line search to obtain an improved step-length. Based largely on the credo of "Look before you leap," the line search is performed on the objective function in the direction indicated by $\tilde{p}$. The line search locates, or approximates the location of, the minimum in this single dimension. The distance to the minimum in this single dimension is taken as the step-length ρ. This minimum is taken as the new estimate of $\tilde{x}$ by taking a step of length ρ in the $\tilde{p}$ direction (Equation 6.13).

The next level of modifications made to Newton's Method involve altering the eigenvalues of the Hessian. The ideal modification will converge rapidly, with speed approaching that of Newton's Method, and will always be descending downhill towards the minimum. A direction of descent is guaranteed if the Hessian is positive definite, meaning that all of the eigenvalues are positive. Three methods are discussed that modify Newton's Method to produce a positive definite Hessian. These are the method of steepest descent, the Marquardt (1963) modification, and the Greenstadt (1967) modification. The method of steepest descent is included primarily for illustrative purposes and is not recommended for practical usage.

6.2.1 The Method of Steepest Descent

The method of steepest descent is perhaps the easiest of the modifications to implement. The method simply replaces the Hessian matrix with the identity matrix, **I**, multiplied by a scalar, μ:

$$\mathbf{H} \leftarrow \mathbf{I}\mu \tag{6.24}$$

This causes the search vector to be directly proportional to the gradient vector. The search vector will therefore take the largest step in the dimension with the largest gradient--hence the name, "steepest descent."

The method of steepest descent will always move in a direction of descent, albeit not very efficiently. The method is notorious for "hemstitching" through valleys--zigzagging form side to side across the valley while making slow progress along the axis of the valley. Therefore, while the method exhibits good stability--it will *always* move downhill--its rate of convergence is extremely slow, sometimes requiring hundreds of iterations to reach the minimum.

6.2.2 The Marquardt Modification

The Marquardt (1963) modification is based on the principle that adding a constant, μ, to the diagonal elements of the Hessian matrix is equivalent to adding the same constant to the eigenvalues of the Hessian

$$\mathbf{H}+\mathbf{I}\mu \;\leftrightarrow\; \Lambda+\mathbf{I}\mu \tag{6.25}$$

Thus, the Marquardt modification changes the Newton condition to

$$(\mathbf{H} + \mathbf{I}\mu)\,\tilde{p} = -\tilde{g} \tag{6.26}$$

The constant μ, known as the Marquardt parameter, should be chosen so that its addition causes any negative eigenvalues to become positive. If all the eigenvalues are made positive, the Hessian becomes positive definite and a direction of descent is ensured.

Since an analysis of the eigensystem is very expensive, the Marquardt (1963) modification does not actually require knowledge of the eigenvalues. Instead, the Marquardt parameter is initialized as a very large constant. If a line search indicates that extrapolation (an increase in the step-length ρ) is possible, the Marquardt parameter is

reduced by an order of magnitude. On the other hand, if a line search indicates that interpolation (a decrease in the step-length ρ) is necessary, the Marquardt parameter is increased by an order of magnitude.

If the Marquardt parameter is large, the method imitates the method of steepest descent, which converges slowly but has excellent stability properties. If the Marquardt parameter is small, the method behaves like Newton's Method, which has good convergence characteristics but is prone to difficulties. Thus, in ill-conditioned regions the Marquardt (1963) modification will imitate the method of steepest descent whereas in well-behaved areas the method will imitate Newton's Method. The modification seemingly offers the best of both worlds.

The caveat is that the Marquardt (1963) modification can become "stuck" in ill-conditioned regions if the Marquardt parameter is allowed to increase unfettered. Expressing Equation 6.26 as

$$\left(\frac{1}{\mu}\mathbf{H} + \mathbf{I}\right)\tilde{p} = -\frac{1}{\mu}\tilde{g} \tag{6.27}$$

it is apparent that as $\mu \rightarrow \infty$, the step-length becomes infinitesimal. Therefore, when implementing the Marquardt (1963) modification, the Marquardt parameter should always be given an upper bound of some kind and a line search procedure should always be used.

6.2.3 The Greenstadt Modification

Greenstadt (1967) proposed a procedure to ensure that the Hessian matrix is positive definite. The Greenstadt (1967) modification involves two steps:

1) All of the negative eigenvalues are replaced with their absolute value;

2) Any small eigenvalues are replaced with infinity.

The first step requires spectral decomposition to ascertain the eigenvalues. Although this procedure is very expensive computationally, it avoids the main pitfall of the Marquardt (1963) modification--blindly changing the eigenvalues in lockstep. By taking the absolute value of the negative eigenvalues, the Greenstadt (1967) modification merely reverses the direction of the ascending eigenvectors and forces them to take the same step length in a descent direction. The relative proportions of all the eigenvalues are maintained, the only difference being that they are all moving downhill.

The second step of the Greenstadt (1967) modification, replacing small eigenvalues with infinity, is based on the objective function being insensitive to any small eigenvalues. Since the objective function is insensitive to a parameter with a small eigenvalue, this parameter should not be allowed to influence the step-direction. This is precisely what is achieved by replacing the eigenvalue with infinity. Replacing an eigenvalue with infinity is accomplished by replacing the reciprocal of the eigenvalue with zero when inverting the Hessian.

Conceptually, the Greenstadt (1967) modification applied to Newton's Method should result in a robust algorithm that is rapidly convergent and not affected by insensitive parameters; the caveat being that it is very expensive computationally. For information on the performance of the Newton-Greenstadt algorithm applied to petroleum engineering problems, see Barua, Horne, Greenstadt, and Lopez (1989).

6.3 Quasi-Newton Methods

Newton's Method is quadratically convergent when starting with a good initial estimate. However, it is very expensive since the Hessian must be built and solved every iteration, particularly when the Hessian is built with finite difference approximations. The idea behind Quasi-Newton methods is to compromise on the speed of convergence while saving on the expense associated with building and solving the Hessian. Instead of building and solving an exact Hessian every iteration, Quasi-Newton methods attempt to update an approximation of the Hessian.

Quasi-Newton theory is based on multidimensional generalizations of the secant method. The object is to build up secant information as the iterations proceed. Suppose at the kth iteration, the Newton step $\{\tilde{x}_{k+1} - \tilde{x}_k\}$ causes a change in the gradient of $\{\tilde{g}_{k+1} - \tilde{g}_k\}$. Then the next Hessian approximation will satisfy the secant passing through these two iterates if

$$\tilde{x}_{k+1} - \tilde{x}_k = \mathbf{H}_{k+1} (\tilde{g}_{k+1} - \tilde{g}_k) \tag{6.28}$$

This condition is termed the Quasi-Newton condition and is the design criteria for Quasi-Newton methods. Notice the similarity between this condition and the Newton condition, Equation 6.12. This condition forces the Hessian approximation to exactly match the gradient of the function in the displacement direction, $\{\tilde{x}_{k+1} - \tilde{x}_k\}$. For multiple

dimensions, it is impossible to uniquely solve for the Hessian approximation, since there are an infinite number of solutions that will satisfy the Quasi-Newton condition. As there are many different Hessian approximations that will satisfy the Quasi-Newton condition, there are equally many Quasi-Newton methods. All of these attempt to update the current Hessian approximation rather than build a new one from scratch.

The Broyden, Fletcher, Goldfarb, Shanno (BFGS) method (Broyden, 1970) is particularly suitable for optimization. Using the notation

$$\tilde{y}_k \equiv \tilde{g}_{k+1} - \tilde{g}_k \tag{6.29}$$

$$\tilde{s}_k \equiv \tilde{x}_{k+1} - \tilde{x}_k \tag{6.30}$$

the BFGS update may be written as

$$\mathbf{H}_{k+1} = \mathbf{H}_k + \frac{\tilde{y}_k \tilde{y}_k^T}{\tilde{y}_k^T \tilde{s}_k} - \frac{\mathbf{H}_k \tilde{s}_k \tilde{s}_k^T \mathbf{H}_k}{\tilde{s}_k^T \mathbf{H}_k \tilde{s}_k} \tag{6.31}$$

Starting with the identity matrix, the Hessian approximation is built up as the iterations proceed. This update maintains the symmetry and positive definiteness of the Hessian approximation while satisfying the Quasi-Newton condition. Most importantly, the BFGS update requires fewer function evaluations than Newton's Method.

The drawback of using a Quasi-Newton method such as the BFGS update is that the convergence is q-superlinear (somewhere in between linear and quadratic convergence). The hope is that the reduced cost of each iteration makes up for the reduced rate of convergence and the overall method is more efficient than Newton's Method.

6.4 The Polytope Algorithm

All of the aforementioned methods are some variation of Newton's Method. These methods require a smooth, continuous function that is twice differentiable. Complications arise if these derivative-based methods are used on nonsmooth functions. Fortunately, there are alternative methods available that do not require derivative information. These alternative methods are called direct search methods or function comparison methods. They require nothing more than the value of the objective function at several different points and are equally applicable to smooth and nonsmooth functions. The concept of the

direct search method is simple to understand but sometimes challenging to implement. Furthermore, due to the heuristic nature of direct search methods, no guarantee can be made of their convergence.

The polytope algorithm (Gill, 1983) is a good example of a function comparison method. For a problem consisting of *n* decision variables, a polytope of *n*+1 points is created. The objective function is evaluated at each point and then the polytope moves away from the point with the largest value by replacing it with a new point on the opposite side of the polytope. This is the reflected point. If the reflected point is a "good" point, the polytope attempts to expand in this direction. If the reflected point is a "bad" point, the polytope contracts in size. The polytope moves along, one new function evaluation at a time, reflecting, expanding, and contracting. At the minimum of the function, it should contract to a small enough size to satisfy convergence criteria.

For an *n*-dimensional problem, the polytope consists of *n*+1 points, $\tilde{x}_1$, $\tilde{x}_2$, ..., $\tilde{x}_{n+1}$. The objective function is evaluated at each of the points and the function values, F_1, F_2, ..., F_{n+1}, are ranked such that $F_{n+1} \geq F_n \geq ... \geq F_2 \geq F_1$. The maximum function value, F_{n+1}, and its corresponding point, $\tilde{x}_{n+1}$, are removed from the polytope set. The centroid of the remaining *n* points is given by

$$\tilde{c} = \frac{1}{n} \sum_{j=1}^{n} \tilde{x}_j \tag{6.32}$$

The centroid is used to generate the trial reflection point (see Figure 6.3)

$$\tilde{x}_r = \tilde{c} + \alpha(\tilde{c} - \tilde{x}_{n+1}) \tag{6.33}$$

where α is the reflection coefficient ($\alpha \approx 1$). Evaluating the function at $\tilde{x}_r$ yields F_r. There are three possibilities for the reflected function value, F_r, when compared to the existing set of function values: 1) it is the new low value, 2) it is the new high value, or 3) it is somewhere in between:

1) $F_r < F_1$. If the reflection function value is the new low value, then we assume that this is a "good" direction and attempt to expand the polytope even further along the reflection vector. The expansion point, $\tilde{x}_e$, is given by

$$\tilde{x}_e = \tilde{c} + \beta(\tilde{x}_r - \tilde{c}) \tag{6.34}$$

where β is the expansion coefficient ($\beta > 1$). The expansion value, F_e, is obtained at $\tilde{x}_e$. If $F_e < F_r$ then the expansion has been successful and $\tilde{x}_e$ replaces $\tilde{x}_{n+1}$. If the expansion failed then $\tilde{x}_r$ replaces $\tilde{x}_{n+1}$.

2) $F_r > F_n$. If the reflection value is larger than the largest value in the set, the polytope is assumed to be too large and is contracted. The contraction point, $\tilde{x}_c$, is given by

$$\tilde{x}_c = \tilde{c} + \gamma(\tilde{x}_{n+1} - \tilde{c}) \qquad \text{if } F_r \geq F_{n+1} \tag{6.35}$$

$$\tilde{x}_c = \tilde{c} + \gamma(\tilde{x}_r - \tilde{c}) \qquad \text{if } F_r < F_{n+1} \tag{6.36}$$

where γ is the contraction coefficient ($0 < \gamma < 1$). The contraction value, F_c, is obtained at $\tilde{x}_c$. If $F_c < \min\{ F_r, F_{n+1} \}$ then the contraction step has succeeded and $\tilde{x}_{n+1}$ is replaced by $\tilde{x}_c$. Otherwise, an additional contraction is performed.

3) $F_1 \leq F_r \leq F_n$. If the reflected function value is not the new low value or the new high value then the reflection point, $\tilde{x}_r$, is added to the set of points and replaces $\tilde{x}_{n+1}$.

Thus, $\tilde{x}_{n+1}$ is replaced with either $\tilde{x}_r$, $\tilde{x}_e$, or $\tilde{x}_c$ and a new iteration is commenced.

In addition to reflecting, contracting, and expanding, the polytope algorithm also includes restarting and shrinking. Restarting involves creating a new polytope whose vertices are equidistant from the current centroid. Restarting is necessary if the polytope becomes unbalanced after several cycles of contracting and expanding in different dimensions. Restarting is also necessary if the polytope begins to oscillate back and forth between the same points, reflecting from one side of the polytope to the other. Shrinking the polytope is necessary if a contraction step fails or if the best point remains unchanged for too many iterations. Shrinking the polytope involves moving all of the vertices towards the best point by some fraction.

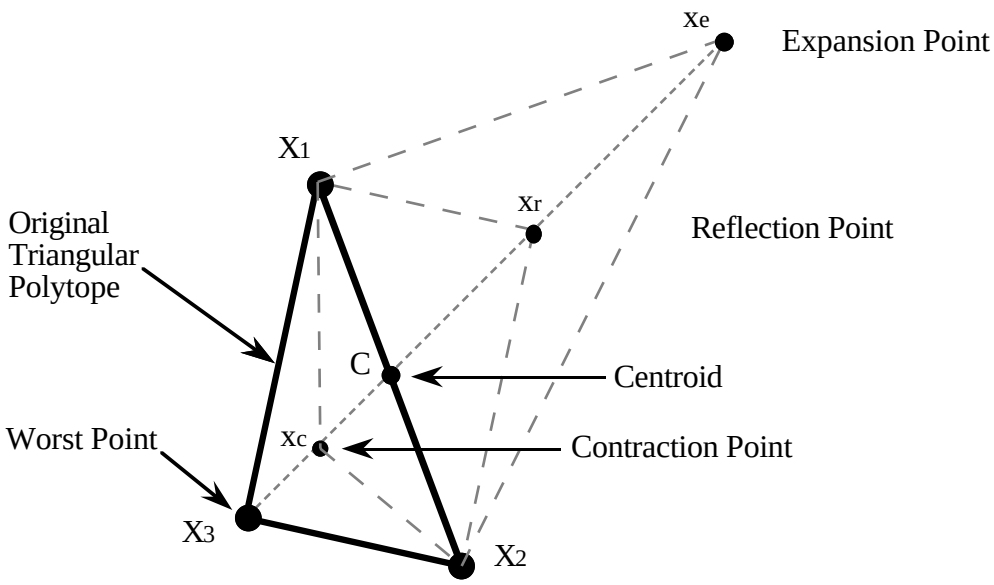

Figure 6.3: Two-Dimensional Polytope with Reflection, Expansion, and Contraction Points.

One of the difficulties with the polytope algorithm is distinguishing between when the algorithm is undergoing temporary difficulty and when it has found the minimum. Nelder and Mead (1965) suggest the following two stopping criteria

$$\text{Criterion 1:} \qquad |F_1 - F_{n+1}| \le \varepsilon (1 + |F_1|) \tag{6.37}$$

$$\text{Criterion 2:} \qquad \sum_{i=1}^{n+1} \left(F_i - \frac{\sum_{j=1}^{n+1} F_j}{n+1} \right)^2 \le \varepsilon \tag{6.38}$$

where ε is a specified tolerance. The method is assumed to have converged as soon as one of the two criteria has been satisfied.

While the polytope algorithm will never be as robust as a derivative-based method, it can be useful for a nonsmooth, nondifferentiable function where a derivative-based method would fail. On a smooth function, the polytope algorithm will always be slower to converge and less reliable, especially in higher dimensions. If the polytope algorithm is

employed, significant enhancements can be made to the polytope algorithm on a case-by-case basis.

Chapter 7

RESULTS

Each of the preceding chapters has expounded the theory of a single facet of the well model. This chapter will discuss how this study integrated each of these individual components into a functional production system model and how the production system model was then optimized.

7.1 Model Development

7.1.1 Developing a Well Model Prototype

To test out the general concept of using numerical techniques to optimize a well model, a simplified well model was initially developed. The simplified model was a single-phase, dry-gas model that consisted of three distinct components: a generalized inflow performance relationship to model the reservoir deliverability; the Cullender and Smith (1956) correlation to model the flow in the vertical tubing; and the Weymouth equation to model the flow through a horizontal flowline. The well components were coupled together and optimized with Newton's Method. The decision variables of tubing inside-diameter and flowline inside-diameter were used to optimize the objective criterion of instantaneous flow rate (see Figures 7.1 and 7.2). Due to the simplified nature of the model, the surface was unbounded--the larger the inside-diameters, the larger the flowrate. The inside-diameters were constrained to be a maximum of five inches each. Figure 7.3 shows the convergence path for two different starting points, both of which converge to the maximum inside-diameters allowed.

Having proven the general concept of production optimization on a prototype, a more ambitious model-development program was launched. The new well model was to have significant improvements over the initial model. The new model was to account for multiphase flow in the reservoir, in the tubing, and in the surface facilities. The reservoir component of the new model was to account for the reservoir performance over time. The new model was to model flow through the surface choke, have an optimization scheme

Figure 7.1: Flow Rate Surface of Single-Phase Model, 3-D.

Figure 7.2: Flow Rate Surface of Single-Phase Model, 2-D.

Figure 7.3: Convergence Path of Single-Phase Model.

more stable than unmodified Newton's Method, and was to optimize long-term financial objectives.

7.1.2 Developing the Reservoir Component

To replicate the reservoir dynamics and inflow performance in the well model, this study adopted a reservoir model developed by Borthne (1986) at the Norwegian Institute of Technology, as discussed in Chapter 2. The reservoir model was originally designed with just this purpose in mind--to provide a simple but functional reservoir component to be included in a larger model. The model provides an accurate representation of constrained reservoir performance that requires minimal computer processing. Borthne's model is a black-oil model that performs a generalized material balance calculation in concert with an inflow performance relationship based on pseudopressure. The reservoir model is constrained by both pressure and flowrate. In addition to specifying a minimum flowing well pressure, two flowrates must be specified: a minimum flowrate and a maximum target flowrate. The model attempts to satisfy the target flowrate without violating the minimum flowing well pressure. For more details on the reservoir component used in the well model, see Chapter 2.

7.1.3 Developing the Tubing Component

The next stage in the model development was to design and develop a component to model the multiphase flow through the vertical flowstring. For this we relied on the many empirical correlations that have been developed over the years. Three correlations were selected to be included in the model. These were the modified Hagedorn & Brown correlation (1965), the Orkiszewski correlation (1967), and the Aziz, Govier, and Fogarasi correlation (1972). All three correlations are extensively used in the petroleum industry. The Hagedorn and Brown (1965) correlation is one of the most empirical available, the Aziz *et al.* (1972) correlation has the strongest theoretical basis.

Gradient maps of the three correlations were generated and are shown in Figures 7.4 through 7.9. Figures 7.4 and 7.5 show the gradient surface generated by the modified Hagedorn and Brown (1965) correlation. The transition from the original Hagedorn and Brown correlation, representing slug flow, to the Griffith & Wallis (1961) correlation, representing bubble flow, is very distinct. Figures 7.6 and 7.7 show the Aziz *et al.* (1972) correlation with their suggested flow map superimposed. Note theat the map appears continuous everywhere except at the boundary between bubble flow and slug flow.

Figure 7.4: Hagedorn and Brown Gradient Map, 2-D.

Figure 7.5: Hagedorn and Brown Gradient Map, 3-D.

Figure 7.6: Aziz, Govier, and Fogarasi Gradient Map, 2-D.

Figure 7.7: Aziz, Govier, and Fogarasi Gradient Map, 3-D.

Figure 7.8: Orkeszewski Gradient Map, 2-D.

Figure 7.9: Orkeszewski Gradient Map, 3-D.

The Orkiszewski gradient maps appear in Figures 7.8 and 7.9. Here the boundaries between all four flow regions are very distinct. For more information on the multiphase flow component used in this well model, see Chapter 3.

7.1.4 Developing the Choke Component

After the reservoir and flowstring components were completed, we next developed a component to model the surface choke. A surprising degree of difficulty was encountered at this stage. Recall from Chapter 4 that a surface choke is a binary device: it operates in either critical flow or subcritical flow. Also recall that in critical flow the flow rate through the choke is independent of the downstream pressure. Thus a discontinuity occurs at the critical-subcritical flow boundary. Since the well model was to be used in an iterative fashion, the surface choke component would have to be applicable to all flow conditions, both critical and subcritical. Much to our dismay, we discovered after researching the techniques available that although good correlations are available for single phase flow across chokes, good correlations for multiphase flow across chokes are rare. Of the correlations that are available, most are strictly for critical flow.

Nodal analysis handles the surface choke discontinuity by avoiding it. In nodal analysis, the separator pressure is specified and then related to the pressure downstream of the choke by a horizontal flow correlation. Then the pressure drop across the choke is obtained by assuming that the choke is always in critical flow and using an empirical correlation. Notice that by specifying the downstream pressure and then calculating the upstream pressure, this procedure manages to determine both the upstream and downstream pressures in critical flow. If we specified the upstream pressure and tried to determine the downstream pressure during critical flow, the best we can do is to ascertain the maximum downstream pressure.

Assuming that the choke is always in critical flow was rejected as an option for this well model. An attempt was made to devise a method to handle both critical and subcritical flow. One of the few correlations to make an attempt at modeling both critical and subcritical flow is the Sachdeva *et al*. (1986) choke model. With a few modifications to the algorithm, the Sachdeva *et al*. (1986) model was able to be incorporated into the well model. During critical flow through the choke, the downstream pressure was determined by assuming the choke to be at the critical-subcritical boundary. This assumption allowed the critical pressure ratio to determine the downstream pressure. See Chapter 4 for details.

The Sachdeva *et al*. (1986) model was developed and tested with the other components of the well model. Figure 7.10 shows the present value surface generated by the Sachdeva *et al*. (1986) model as a function of choke diameter and tubing diameter. Notice that the critical-subcritical flow boundary occurs at a choke diameter of approximately ten centimeters. Below this critical size, the surface is completely a function of the choke diameter. Above the critical choke diameter, the surface is completely a function of the tubing diameter. However, a physical constraint is required: the choke diameter cannot be allowed to exceed the tubing diameter. This constraint is shown in Figure 7.11.

Although we were able to successfully incorporate into the well model a choke component that modeled both critical and subcritical flow, this was at great computational expense. In addition, several of the assumptions in the choke model, such as no mass transfer occurring between phases, were considered to be highly suspect. For these reasons, we opted not to include a choke component in the well model.

7.1.5 Developing the Separation Component

The next stage was the development of a component to model surface facilities. We elected to model the surface facilities with a two-stage separation process. A two-stage separation process involves flashing the well stream initially at the separator operating conditions and then flashing the resulting liquid stream at stock tank conditions. The flash calculation implemented in this component is based on the Soave-Redlich-Kwong equation of state. For more information on the phase separation component, see Chapter 5.

Thus, in its final state, the well model consists of a reservoir component, a production string component, and a surface phase separation component. For any combination of variables, the model will give the production profile for a given time step and a given project life. In all examples cited here, a six-month time step and a 15 year project life was used.

7.2 Defining the Objective Criterion

In order to perform optimization on the well model, the production profile had to be transformed into an objective criterion. The objective criterion used in this research was the

Figure 7.10: Present Value Surface of Choke Diameter vs. Tubing Diameter.

Figure 7.11: Constrained Present Value Surface of Choke Diameter vs. Tubing Diameter.

present value of the revenue stream generated over the life of the project. The present value of the revenue stream is obtained by discounting the revenue stream over the life of the project back to the present. The discounting scheme used in this model is relatively simple and easy to follow. The model accounts for both the company's cost of capital and the expected inflation rate. Both of these parameters are assumed constant over the life of the project.

A company has two primary means of securing capital from outside sources: the issuance of equity in the company and the assumption of debt. A company's cost of capital is typically determined as a weighted average of the company's cost of debt and the company's cost of equity. If we let

r_D = interest rate of debt, fraction

r_E = return on equity expected by shareholders, fraction

D = amount of long-term debt, $

E = amount of outstanding equity, $

T_C = corporate tax rate, fraction

then the company's cost of capital may be expressed as

$$r^* = r_D (1 - T_C) \frac{D}{D+E} + r_E \frac{E}{D+E} \qquad (7.1)$$

Typically a company's executive management will specify the weighted-average cost of capital to be used in financial calculations.

Knowing the cost of capital, r*, and the inflation rate, i, the discount rate, in real terms, may be expressed as

$$R = \frac{(1+r^*)}{(1+i)} - 1 \qquad (7.2)$$

Thus both the effect of the cost of capital and the effect of inflation have been coupled into one discount factor. Note that this discount factor, the real discount factor R, may only be used with cash flow expressed in real terms.

At the end of each time step, the well model gives the cumulative production that occurred during a time step. Specifically, the well model will yield a stream of *n* production quantities, C_1, C_2, ..., C_n, where *n* is the number of time steps occurring over the life of the project. These production quantities are discounted back to the present by assuming the production is constant over the time step and discounting from the midpoint of the time step (see Figure 7.12).

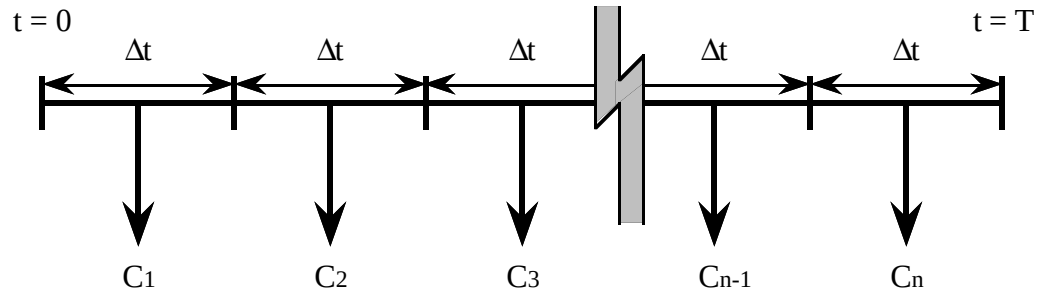

Figure 7.12: Revenue Stream is Discounted from Center of Time Step.

For instance, if the time step is one year, then the cumulative production produced over the first year will be discounted as if it were sold in one discrete quantity at six months' time. Thus, the present value of the production stream for *n* time steps of length Δt may be expressed as

$$PV = \sum_{T=1}^{n} \left[\frac{C_n P_n}{(1+R)^{((2n-1)/2)\Delta t}} \right] \qquad (7.3)$$

where P_n is the real price of the production at the *n*th time step.

The present value calculation determines only the positive effects of the decision variables, namely the revenue stream. The concept of present value is easy to conceptualize since it is simply the gross value of the revenue stream. To change the objective criterion from present value to net present value, the negative effects of the decision variables must be included. For instance, the negative effects may include capital expenditure, tax payments, royalty payments, labor cost, and corporate overhead contribution just to name a few. Since the purpose of the research was to demonstrate the effective application of optimization techniques and not to concoct an elaborate economic model, present value was made the objective criterion. However, to use this technique in the design or analysis of an actual well system, the objective criterion should be made to reflect the financial

ramifications as accurately as possible and therefore a criterion of net present value should be used.

7.3 Results

7.3.1 The Surface of the Well Model

Once the well model was completed and the objective criterion was decided upon, a surface map was generated of the objective criterion as a function of two decision variables. Namely, the present value of the production stream was plotted as a function of the separator pressure and the tubing diameter (see Figure 7.13). The surface appears to be a textbook example of an optimization surface: nice, smooth contour lines bounding the extreme value on all sides. However, closer inspection of the surface reveals a different story. As shown in Figure 7.14, looking at a closer level reveals a surface that is very rough and ill-behaved. The rough features were masked by the graphics software in Figure 7.13 but are plainly visible in Figure 7.14.

A better understanding of the surface can be obtained by examining several unidimensional profiles. Figures 7.15 through 7.18 show four different profiles of the surface. The first three figures keep the separator pressure constant while varying the tubing diameter. It is clearly visible that the surface is very rough and discontinuous along this dimension. Figure 7.17 shows the amount of noise present at the maximum of the surface. Figure 7.18 is a profile of the other dimension. This profile was obtained by holding the tubing diameter constant and varying the separator pressure. The figure shows that in this dimension, the surface is a very smooth and continuous function. Thus, the surface is rough as a function of tubing diameter and smooth as a function of separator pressure.

This conclusion about the surface obtained from the profiles is reinforced by investigating the derivatives of the function. Figures 7.19 and 7.20 show the first and second derivatives of separator pressure. These derivatives clearly exhibit that the surface is very smooth as a function of separator pressure (be advised that the two graphs are shown from two different viewing angles). The smoothness of the function with respect to separator pressure is very much in contrast to the roughness of the function with respect to tubing diameter. Figures 7. 21 and 7.22 show the first and second derivatives of tubing

Figure 7.13: Present Value Surface of Separator Pressure vs. Tubing Diameter.

Figure 7.14: Rough Features of Present Value Surface.

Figure 7.15: Profile of Tubing Diameter for Constant Separator Pressure.

Figure 7.16: Close-up of Tubing Diameter Profile for Constant Separator Pressure.

Figure 7.17: Close-up of Tubing Diameter Profile at Optimum.

Figure 7.18: Profile of Separator Pressure for Constant Tubing Diameter.

Figure 7.19: First Derivative of Separator Pressure.

Figure 7.20: Second Derivative of Separator Pressure.

Figure 7.21: First Derivative of Tubing Diameter.

Figure 7.22: Second Derivative of Tubing Diameter.

Figure 7.23: Second Mixed-Partial Derivative of Tubing Diameter and Separator Pressure.

diameter (again the graphs are shown from two different angles). The surface is very discontinuous in the vicinity of the optimal tubing diameter. Figure 7.23 shows the second mixed partial derivative. Note that the origin of this derivative coincides with the extreme value of the surface.

Further insights to the function can be obtained by investigating the eigensystem of the surface. Figures 7.24, 7.25, and 7.26 show the minimum eigenvalue of the surface, the maximum eigenvalue of the surface, and the curvature of the surface. Notice that the eigenvalues are negative. Going against the convention in optimization to always pose the problem so that minimization is performed, this study has explicitly performed maximization of the objective function by using a negative definite Hessian. Since the Hessian is forced to be negative definite so that an *ascent* direction is assured, the eigenvalues are negative in value. Since we are approximating the objective function with a negative definite Hessian, regions of positive curvature indicate areas where Newton's Method may fail to converge. Note the similarity between these three graphs and the three graphs of the second derivatives.

7.3.2 Performing Optimization on the Well Model

Having developed the well model and having analyzed the properties of the surface of the decision variables, numerical optimization techniques were employed in an attempt to maximize the function. Knowing that the surface is not smooth with respect to one of the variables, we did not expect derivative-based optimization methods to perform very well on the function.

Figure 7.27 shows the results of using unmodified Newton's Method to optimize the function. Shown on the figure are four different starting points that are all relatively close to and equidistant from the desired solution. However, two of the starting points resulted in convergence to the maximum value while two of the starting points resulted in divergence. The difference between the four points becomes apparent by analyzing Figure 7.21, the graph showing the first derivative of the tubing diameter. Figure 7.21 shows a trough occurring in the first derivative between a tubing diameter of eight to nine centimeters. The trough in the first derivative of the tubing diameter represents an inflection of the second-order surface. In essence this trough divides two distinct second order surfaces. The two points that converged to the maximum were on one side of this inflection while the two points that diverged were on the other side of the inflection. Recall from Chapter 6 that unmodified Newton's method simply makes a quadratic approximation

Figure 7.24: Minimum Eigenvalue of Hessian Matrix.

Figure 7.25: Maximum Eigenvalue of Hessian Matrix.

Figure 7.26: Curvature of Hessian Matrix.

to whatever the immediate second order surface happens to be. Since unmodified Newton's method does not force the solution to take a descent direction, the two points which start at a tubing diameter of nine centimeters are attempting to converge to a stationary point other than the desired stationary point. Thus, using unmodified Newton's Method, the initial guess must be on the proper side of this inflection to converge to the desired stationary point.

We next tried optimizing the function with a modified form of Newton's Method. The algorithm employed was obtained from Dr. Walter Murray of the Stanford Optimization Laboratory. The algorithm is described on pages 108-111 of Gill *et al*. (1981) and is based on modified Cholesky factorization. The modification is very similar to the Greenstadt modification discussed in Chapter 6 in that after it factors the Hessian to obtain the diagonal, it forces the diagonal elements to be positive and greater than some small value. The algorithm also employs a line search procedure to ensure that the optimal step length is taken for a given search direction. As can be seen from Figure 7.28, significant improvement was achieved in the convergence to the maximum value. Even when the starting points were not near the solution, the method always converged to the optimum solution.

Due to the unavailability of analytic derivatives, both of the Newton-based methods determined the gradient and Hessian by using finite difference approximations. Since the surface of the function is nonsmooth, obtaining meaningful derivatives was very difficult. Critical in the performance of both methods was the size of the finite difference interval. By taking relatively large finite difference intervals, we were able to mask the effects of the nonsmooth surface. We found that taking finite differences of one-tenth of the size of the decision variables produced good results.

As an alternative to derivative-based methods, the performance of the polytope heuristic was investigated. As discussed in Chapter 6, the polytope heuristic is a direct search method based on function comparisons and not on derivative information. The performance of the polytope heuristic is shown in figures 7.29, 7.30, and 7.31. Measured strictly on the number of function evaluations required to find the solution, the polytope method took the equivalent of five iterations of Newton's Method. Specifically, the convergence path shown in Figure 7.29-7.31 required 45 function evaluations which is equivalent to five iterations of a Newton-based method using a nine-point finite differencing scheme.

Figure 7.27: Convergence Path of Unmodified Newton’s Method.

Figure 7.28: Convergence Path of Modified Newton’s Method.

Figure 7.29: Convergence Path of Polytope Heuristic, 2-D.

Figure 7.30: Convergence Path of Polytope Heuristic, 3-D.

Figure 7.31: Convergence Path of Triangular Polytopes.

Chapter 8

CONCLUSIONS

8.1 Conclusions

The emphasis of this study may be summarized by two key points:

1) Nonlinear optimization techniques can be successfully applied to production system optimization.

2) Nonlinear optimization of a production system model is an intelligent alternative to exhaustive iteration of a production system model.

The significant advantages of using nonlinear optimization in lieu of exhaustive iteration are

- Nonlinear optimization is not limited by the number of decision variables--an unlimited number of decision variables may be optimized simultaneously. Exhaustive iteration is limited to one or two decision variables and becomes intractable when three or more variables are optimized, especially when the variables are interrelated.

- Nonlinear optimization may be used to optimize various objective criteria. Examples of various objective criteria are: to maximize the present value of the production stream, to maximize the net present value of the well, to maximize cumulative recovery on an equivalent barrel basis, to minimize the cumulative gas-oil ratio, to minimize the cumulative water-oil ratio, to minimize total investment per equivalent barrel produced, to maximize the rate-of-return of the well, etc.

- Nonlinear optimization may be used to optimize well conditions over a span of time. This is best described by considering an example: for a ten-year time span, nonlinear optimization will determine the optimal tubing diameter to use each year--simply add ten decision variables, one for each tubing size each year. As another example, if only three tubing changes are allowed over the ten-year span, nonlinear optimization will determine when the changes should be made and what size the tubing should be. Attempting this with exhaustive iteration is ill-advised.

- Nonlinear optimization avoids the trial and error procedure of exhaustive iteration. Nonlinear optimization based on Newton's technique will achieve quadratic convergence to the optimal solution.

This study investigated several different nonlinear optimization methods. The significant findings are

- Unmodified Newton's Method is not viable for optimization. This technique is highly sensitive to the initial guess.

- The performance of Newton's Method can be greatly improved by including a line search procedure and a modification to ensure a direction of descent.

- For nonsmooth functions, the polytope heuristic provides an effective alternative to a derivative-based method.

- For nonsmooth functions, the finite difference approximations are greatly affected by the size of the finite difference interval. This study found a finite difference interval of one-tenth of the size of the variable to be advisable.

8.2 Suggestions for Future Work

One idea that was flirted with briefly but is not included in this report is to revise the implementation of classical nodal analysis. Current practitioners of nodal analysis use exhaustive iteration to solve the system of equations that represents the well. Why not

formulate the problem to solve for the root of a system of nonlinear equations, namely by using Newton's Method? Simply set up the problem to contain a pressure residual at each node and then use Newton's Method to solve the equations for the stabilized flow rate. Alternately, you could set up the problem to contain a flow rate residual at each node and then use Newton's Method to solve the equations for the stabilized pressure at the solution node. Hence, you could use Newton's Method for two different purposes in the optimization of a production system: to solve for the zero of the function and then again to solve for the zero of the gradient of the function.

Several improvements can be made to the current well model. Obviously, it would be interesting to know why the model is nonsmooth with respect to tubing diameter. The cause of this is not yet apparent. In addition, it would be nice to expand the model to include a completion component that models the completion effects (perforations, gravel pack, ...) and also a horizontal flow component that models the pressure loss and phase segregation that occur in surface flowlines between the wellhead and the separator. It would also be interesting to develop a well model based on a compositional equations instead of black oil equations. In addition, one area where the current well model has significant problems is with computational expense. A more efficient manner for solving for the stabilized flow rate should be found.

Perhaps the biggest improvement would be to demonstrate the use of different objective criteria in the optimization process. This would clearly demonstrate the inherent advantages of nonlinear optimization over exhaustive iteration.

Nomenclature

A	Area.
B	Flow regime boundaries used by Aziz *et al* (1972) correlation.
B_α	Formation volume factor of phase α.
C	Centroid of polytope; Hagedorn and Brown (1965) correlating parameter.
C_D	Discharge coefficient.
C_v	Cumulative production during time step n.
D	Diameter; Long-term debt, $; Non-Darcy skin.
ΔE	Material balance error.
Δt	Time step, $t_k - t_{k-1}$.
E	Outstanding equity, $.
e_i	ith unit vector.
E_K	Kinetic energy component; acceleration term.
F	Nonlinear function.
f_α	Fugacity of phase α; Fractional flow rate of phase α.
f_M	Moody friction factor.
$\hat{f}$	Partial fugacity.
G	Cumulative gas production; Mass flux.
g	Force of gravity; Gradient *n*-vector of x.
g_c	Gravity constant.
H	Hessian matrix.
H_α	Holdup of phase α; Enthalpy of phase α.
h	Height of reservoir.
h_i	Finite difference interval of ith dimension.
I	Identity matrix.
i	Inflation rate, fraction.
K	Specific heat ratio, Cp / Cv; Equilibrium ratio; Binary interaction parameter.
k	Reservoir permeability.
$k_{r\alpha}$	Relative permeability of phase α.
L	Flow regime boundary used by Griffith & Wallis (1961), Orkiszewski (1967); Liquid mole fraction.
λ_α	No-slip holdup of phase α.
M	Mobility ratio.
m	Mass of fluid in the reservoir.

m(P)	Gas pseudopressure.
N	Cumulative oil production; Dimensionless groups defined by Ros (1961); Flow regime parameter used by Aziz *et al*. (1972).
P	Pressure; The *n*-vector of displacement from x; Newton search vector.
P_n	Real price of the production at the *n*th time step
PV	Present value.
Q	Quadratic equation.
Q*	Stabilized flow rate determined by nodal analysis.
q	Volumetric flow rate.
$\tilde{q}$	Mass flow rate.
R	Universal gas constant; Real discount factor.
r*	Cost of capital, fraction.
r_D	Interest rate of debt, fraction.
Re	Reynold's number.
r_E	Return on equity expected by shareholders, fraction.
re	Radius of drainage.
R_P	Producing gas-liquid ratio.
R_S	Solution gas-oil ratio.
r_S	Solution oil-gas ratio.
r_w	Radius of wellbore.
S	Darcy skin; Diameter of bean, 64ths of an inch.
S_α	Saturation of phase α.
T	Temperature.
T_C	Corporate tax rate, fraction.
V	Volume; Velocity; Specific volume; Vapor mole fraction; Matrix of eigenvectors.
V_α	Velocity of phase α.
V_B	Bulk volume of the reservoir.
V_{BF}	Absolute bubble rise velocity.
V_{BS}	Bubble rise velocity.
V_M	Superficial velocity of the mix.
$V_{S\alpha}$	Superficial velocity of phase α.
ω_α	Acentric factor of phase α.
X	Free gas quality; Oil composition.
x	n-vector of decision variables.
x_c	Contraction point.

x_e	Expansion point.
x_r	Reflection point.
Y	Pressure ratio, downstream to upstream pressure; Composition of gas.
Z	Objective variable; depth in well; Composition of mixture.

Subscripts

1	Upstream.
2	Downstream.
BUB	Bubble flow regime.
c	Critical.
CH	Choke.
F	Friction.
G	Gas.
GG	Gas phase derived from gas phase.
GO	Gas phase derived from oil phase.
HB	Hagedorn and Brown.
HH	Hydrostatic head.
i	Gridblock position in x-direction.
j	Gridblock position in y-direction.
K	Iteration number.
KE	Kinetic energy.
L	Liquid.
M	Mixture.
MIST	Annular-mist flow regime.
NS	No slip.
O	Oil.
OG	Oil phase derived from gas phase.
OO	Oil phase derived from oil phase.
r	Reduced.
S	Slip.
SLUG	Slug flow regime.
TRANS	Transition flow regime.
W	Water.
WE	Weber.
WH	Wellhead.

Superscript.

“	Variable is normalized to reservoir bulk volume.
L	Liquid phase.
R	Reservoir conditions.
S	Standard conditions.
T	Transpose.
V	Vapor phase.

Greek Letters

α	Reflection coefficient.
β	Expansion coefficient .
ε	Absolute pipe roughness; tolerance.
ϕ	Reservoir porosity; Fugacity coefficient.
Φ_α	Mechanical irreversibilities of phase α.
γ	Contraction coefficient.
Λ	Diagonal matrix of eigenvalues.
μ	Marquardt parameter.
μ_α	Viscosity of phase α.
ρ	Newton step length.
ρ_α	Density of phase α.
σ	Interfacial tension.
ψ	Hagedorn and Brown correlating parameter; Roots of cubic equation.
∇	Gradient.
$\nabla\cdot$	Divergence.

Bibliography

[1] Achong, I.: “Revised Bean Performance Formula for Lake Maracaibo Wells,” Shell Internal Report (Oct. 1961).

[2] Ali, H. M., Batchelor, A.S.J., Beale, E.M.L., and Beasley, J.F.: “Mathematical Models to Help Manage the Oil Resources of Kuwait,” unpublished manuscript (1983).

[3] Amyx, J. W., Bass, D. M., and Whiting, R. L.: *Petroleum Reservoir Engineering*, McGraw-Hill, New York (1960).

[4] Arnold, K., and Stewart, M.: *Surface Production Operations: Design of Oil-Handling Systems and Facilities*, Gulf Publishing, Houston, **1** (1986).

[5] Aronofsky, J. S., and Lee, A. S.: “*A Linear Programming Model for Scheduling Crude Oil Production*,” J. Petro. Tech. (July 1958) 51-54.

[6] Aronofsky, J. S., and Williams, A. C.: “*The Use of Linear Programming and Mathematical Models in Underground Oil Production*,” Mgmt. Sci. **8** (1962) 394-407.

[7] Aronofsky, J. S.: “Optimization Methods in Oil and Gas Development,” paper SPE12295, prepared for the J. Petro. Tech. (July 1983).

[8] Asheim, H. A.: “*Offshore Petroleum Exploration Planning by Numerical Simulation and Optimization*,” Ph.D. dissertation, Dept. of Petro. Eng., University of Texas at Austin (December 1978).

[9] Ashford, F. E., and Pierce, P. E.: “Determining Multiphase Pressure Drops and Flow Capacities in Down-Hole Safety Valves,” *J. Petro. Tech*. (Sept. 1975) 1145-1152.

[10] Attra, H. D., Wise, H. B., and Black, W. M.: “*Application of Optimizing Techniques for Studying Field Producing Operations*,” J. Petro. Tech. (January 1961) 82-86.

[11] Aziz, K., Govier, G.W., and Fogarasi, M.: “Pressure Drop in Wells Producing Oil and Gas,” *J. Canadian Petro. Tech.* (July 1972) 38-48.

[12] Barua, J., Horne, R. N., Greenstadt, J. L., Lopez, L.: “Improved Estimation Algorithms for Automated Type-Curve Analysis of Well Tests,” *SPEFE* (March 1988) 186-196.

[13] Barua, Jawahar.: *A Study of Newton Related Nonlinear Methods in Well Test Analysis, Production Schedule Optimization and Reservoir Simulation*, PhD thesis, Stanford University, (1989).

[14] Baxendall, P. B., and Thomas, R.: “The Calculation of Pressure Gradients in High-Rate Flowing Wells,” *J. Petro. Tech.* (Oct. 1961) 1023-1028.

[15] Baxendall, P. B.: “Bean Performance--Lake Wells,” Internal Report (Oct. 1957).

[16] Beggs, H. D., and Brill, J. P.: “A Study of Two-Phase Flow in Inclined Pipes,” *J. Petro. Tech.* (May 1973) 607-617.

[17] Bohannon, J. M.: “A Linear Programming Model for Optimum Development of Multi-Reservoir Pipeline Systems,” *J. Petro. Tech.* (Nov. 1970) 1429-1436.

[18] Borthne, Gunnar.: *A Simulation Model for Oil and Gas-condensate Production Based on Material Balance and Inflow Performance Calculations*, Norwegian Institute of Technology (1986).

[19] Brill, J. P., and Beggs, H. D.: *Two-Phase Flow in Pipes*, Tulsa (1978).

[20] Brown, K. E., and Lea, James F.: “Nodal Systems Analysis of Oil and Gas Wells,” *J. Petro. Tech.* (October 1985) 1751-63.

[21] Brown, K. E.: *The Technology of Artificial Lift Methods*, **1** and **4**, Penwell Publishing Co., Tulsa (1977).

[22] Broyden, C. G.: “The Convergence of a Class of Double Rank Minimization Algorithms. 2. The New Algorithm,” *J. Inst. Math. Appl.* (1970) 6, 221-31.

[23] Charnes, A., and Cooper, W. W.: *Management Models and Industrial Applications of Linear Programming, Vol. II*, John Wiley & Sons, NY (1961).

[24] Chu, M. H., and Evans, R. D.: "Production System Optimization for Natural Fowing Water Drive Wells," SPE Paper 11582, presented at the 1983 Production Operation Symposium, Oklahoma City, Feb 27 - March 1.

[25] Coats, K. H.: "*An Approach to Locating New Wells in Heterogeneous, Gas Producing Fields*," J. Petro. Tech. (May 1969) 549-558.

[26] Crichlow, H. B.: *Modern Reservoir Engineering--A Simulation Approach*, Prentice-Hall, Englewood Cliffs, NJ (1977).

[27] Cullender, M. H., and Smith, R. V.: "Practical Solution of Gas Flow Equations for Wells and Pipelines with Large Temperature Gradients," *Trans*. AIME (1956) 207.

[28] Duns, H., and Ros, N. C. J.: "Vertical Flow of Gas and Liquid Mixtures in Wells," *Proc., 6th World Petro. Congress* (1963) 451-465.

[29] Fancher, G. H., and Brown, K. E.: "Prediction of Pressure Gradients for Multiphase Flow in Tubing," *SPEJ* (March 1963) 59-69.

[30] Fortunati, F.: "Two Phase Flow Through Wellhead Chokes," SPE Paper 3742 presented at the 1972 SPE European Meeting, Amsterdam, May 17-18.

[31] Gilbert, W. E.: "Flowing and Gas-lift Well Performance," *Drill. and Prod. Prac*., API (1954) 126.

[32] Gill, Philip E., Murray, Walter, and Wright, Margaret H.: *Practical Optimization*, Academic Press, New York (1981).

[33] Golan, M., and Whitson, C. H.: *Well Performance*, IHRDC, Boston (1986).

[34] Govier, G. W., and Aziz, K.: *The Flow of Complex Mixtures in Pipes*, Van Nostrand Reinhold Co., New York City (1972).

[35] Greenstadt, J. L.: "On the Relative Efficiencies of Gradient Methods," *Mathematics of Computation*, **21** (1967) 360-67.

[36] Gregory, M., Aziz, K., and Fogarasi, M.: "Analysis of Vertical Two-Phase Flow Calculations, Crude Oil, Gas Flow in Well Tubing," *J. Canad. Petro. Tech.* (Jan 1980) 86-92.

[37] Griffith, P., and Wallis, G. B.: "Two-Phase Slug Flow," *J. Heat Transfer*, ASME (Aug. 1961) 307-320.

[38] Guzhov, A. J., and Medeiediev, V. F.: "Critical Flow of Two-Phase Liquids Through Wellhead Chokes," *Nieftianoie Xoziastva-Moskva* No. 11 (1962) in Russian.

[39] Hagedorn, A. R., and Brown, K. E.: "Experimental Study of Pressure Gradients Occurring During Continuous Two-Phase Flow in Small-Diameter Vertical Conduits," *J. Petro. Tech.* (April 1965) 475-484.

[40] Hazim, S. H. Al-Najjar, and Nimat, B. Abu Al-Soof: "Alternative Flow-Pattern Maps Can Improve Pressure-Drop Calculations of the Aziz *et al.* Multiphase-Flow Correlation," *SPEPE* (August 1989) 327-334.

[41] Hunt, J. L.: "Production-Systems Analysis for Fractured Wells," *SPEPE* (Nov. 1988) 608-614.

[42] Huppler, J. D.: "*Scheduling Gas Field Production for Maximum Profit*," SPEJ (June 1974) 274-279.

[43] IMSL Inc., *IMSL MATH/LIBRARY User's Manual*, **3**, Chapter 8, IMSL, Houston (1987).

[44] Kuller, R. G., and Cummings, R. G.: "*An Economic Model for Investment and Production for Petroleum Reservoirs*," Am. Econ. Rev. **64** (1974) 66-79.

[45] Lang, Z. X., and Horne, R. N.: "Optimum Production Scheduling Using Reservoir Simulators: A Comparison of Linear Programming and Dynamic Programming

Techniques," SPE Paper 12159, presented at the 1983 SPE Annual Technical Conference and Exhibition, San Francisco, October 5-8.

[46] Lasdon, L., Coffman, P. E., MacDonald, R., McFarland, J. W., and Sepehrnoori, K.: "Optimal Hydrocarbon Reservoir Production Policies," *Operations Research* (Jan. 1986) **34**, 40-54.

[47] Lea, J. F., and Brown, K. E.: "Production Optimization Using a Computerized Well Model," SPE Paper 14121, presented at the SPE 1986 International Meeting on Petroleum Engineering, Beijing (March 1986).

[48] Marquardt, D. W.: "An Algorithm for Least-Squares Estimation of Nonlinear Parameters," *J. SIAM* (June 1963) **11**, No. 2, 431-41.

[49] McFarland, J. W., Lasdon, L., and Loose, V.: "Development Planning and Management of Petroleum Reservoirs Using Tank Models and Nonlinear Programming," *Operations Research* (Mar. 1984) **32**, 270-289.

[50] Murray, J. E., III, and Edgar, T. F.: "*Optimal Scheduling of Production and Compression in Gas Fields*," J. Petro. Tech. (Jan. 1979) 109-116.

[51] Nelder, J. A., and Mead, R.: "A Simplex Method for Function Minimization," *Computer Journal* **7**, 308-313.

[52] O'Dell, P. M., Steubing, N. W., and Gray, J. W.: "*Optimization of Gas Field Operation*," J. Petro. Tech. (April 1973) 419-425.

[53] Omana, R. *et al*.: "Multiphase Flow Through Chokes," SPE Paper 2682 presented at the 1969 SPE Annual Meeting, Denver, Sept. 28 - Oct. 1.

[54] Orkiszewski, J.: "Predicting Two-Phase Pressure Drops in Vertical Pipes," *J. Petro. Tech.* (June 1967) 829-838.

[55] Poettman, F. H., and Carpenter, P. G.: "The Multiphase Flow of Gas, Oil and Water Through Vertical Flow Strings with Application to the Design of Gas Lift Installations," *Drill. and Prod. Prac.,* API (1952) 257-317.

[56] Poettmann, F. H., and Beck, R. L.: “New Charts Developed to Predict Gas-Liquid Flow Through Chokes,” *World Oil* (March 1963) 95-101.

[57] Prausnitz, John M., Lichtenthaler, Ruediger N., and Gomes, Edmundo.: *Molecular Thermodynamics of Fluid-Phase Equilibria*, Prentice Hall, Englewood Cliffs (1986).

[58] Press, W. H., Flannery, B. P., Teukolsky, S. A., and Vetterling, W. T.: *Numerical Recipes: The Art of Scientific Computing*, Cambridge Press, Cambridge (1989).

[59] Ros, N. C. J.: “Simultaneous Flow of Gas and Liquid as Encountered in Well Tubing,” *J. Petro. Tech.* (Oct. 1961) 1037.

[60] Ros, N. C. J.: “An Analysis of Critical Simultaneous Gas-Liquid Flow Through a Restriction and its Application to Flow Metering,” *Applied Sci. Research*, **2** (1960) 374.

[61] Ros, N. C. J.: “Theoretical Approach to the Study of Critical Gas Flow through Beans,” Shell Internal Report (Feb. 1959).

[62] Rosenwald, G. W., and Green, D. W.: “A Method for Determining the Optimal Location of Wells in a Reservoir Using Mixed-Integer Programming,” *SPEJ* (Feb. 1974) 44-54.

[63] Rowan, G., and Warren, J. E.: “*A Systems Approach to Reservoir Engineering, Optimum Development Planning*,” J. Canad. Petro. Tech. (July 1967) 84-94.

[64] Sachdeva, R., Schmidt, Z., Brill, J. P., and Blais, R. M.: “Two-Phase Flow Through Chokes,” SPE Paper 15657, presented at the 1986 SPE Annual Technical Conference and Exhibition, New Orleans, October 5-8.

[65] See, B. A., and Horne, R. N.: “Improved Application of Linear Programming Optimization to Nonlinear Reservoir Simulations Using a Least-Squares Determination of the Influence Functions,” *SPEJ* (Oct. 1983) 717-726.

[66] Soave, G.: *Chem. Eng. Sci.*, **27**, 1197 (1972).

[67] Strang, G.: *Introduction to Applied Mathematics*, Wellesley-Cambridge Press, Wellesley, Mass. (1986).

[68] Tangeren, R. E. *et al*.: "Compressibility Effects of Two-Phase Flow," *J. App. Physics*, **20** (1949).

[69] Wattenbarger, R. A.: "*Maximizing Seasonal Withdrawals from Gas Storage Reservoirs*," J. Petro. Tech. (August 1970) 994-998.

[70] Weymouth equation

[71] Wilson, G. M., and Deal, C. H.: *Ind. Eng. Chem. Fundam.*, **1**: 20 (1962).

APPENDIX

Source Code for Well Model